Radiotoxicity and Decay Heat Comparison of Nuclear Waste Produced by a Thorium or Uranium Fuelled Pebble Bed Reactor

Bachelor Thesis

Rik Bijman

NERA August 2014

Department Radiation Science & Technology
Section Nuclear Energy and Radiation Applications
Faculty of Applied Sciences
Delft University of Technology
Mekelweg 15, 2629 JB Delft
The Netherlands

RADIOTOXICITY AND DECAY HEAT COMPARISON OF NUCLEAR WASTE PRODUCED BY A THORIUM OR URANIUM FUELLED PEBBLE BED REACTOR

Bachelor Thesis

Rik Bijman

August 2014

Supervisors:
Dr. Ir. J.L. Kloosterman
Ir. F.J. Wols

Thesis committee:
Dr. Ir. J.L. Kloosterman
Dr. Ir. D. Lathouwers
Ir. F.J. Wols

ABSTRACT

Investigation is moving increasingly in the direction of nuclear energy, both research on safety and sustainability, CO_2 reduction, are important. One of the most innovative and safe, so called Generation IV, reactor designs is the pebble bed reactor design (PBR). Graphite balls contain the fuel, the graphite acts as moderator and helium gas is used as coolant. Both thorium and uranium can be used as fuel.

In this work, comparisons on the nuclear waste produced by a thorium and an uranium fuelled PBR were made. Thorium has some theoretical advantages, e.g. it is three to four times more abundant. It is claimed as well that the thorium cycle produces less minor actinides than the uranium cycle. The aim of this work is to proof this claim and to discover which of the two fuel cycles produces the least radiotoxicity and decay heat, which is important for the storage of the waste. The possible reduction of the radiotoxicity and decay heat production is also analysed in this work by simulations of the effect of recycling of some highly radiotoxic minor actinides.

Using MATLAB and SCALE6 models, simulations were done to compare the radiotoxicity and decay heat production in case of uranium fuelled pebble bed reactors and thorium PBR's both with and without recycling. In order to obtain equivalent configurations for both fuel cycles, they were compared on k_{inf} over the burn-up domain by equalling the average k_{inf}.

It is found that the radiotoxicity production is lower for the thorium fuel cycle, due to the lower production of higher minor actinides because several more neutron captures must occur. The same conclusion can be drawn on short term heat production, which makes the thorium fuel cycle more favourable than the uranium fuel cycle. However, between 100 and 100000 years the heat production in the thorium cycle tends to grow again, which might require sophisticated (and expensive) storage.

For the thorium fuel cycle, it can be concluded that recycling of some highly radiotoxic and heat producing minor actinides can counter this second growth of heat production as well as it decreases the total produced radiotoxicity. Overall, the thorium fuel cycle is most favourable for both long and short term storage.

ACKNOWLEDGEMENTS

First of all I want to thank my daily supervisor, Frank, that I could always just walk by and ask you a question or ask you for your opinion. Thanks for all your tips, ideas and insights during my whole Bachelor project. The comments at your scripts, I used, were also very useful and made it possible to understand what I did and had to improve. I will also miss the nice World Cup and Tour de France analysis that we had during coffee and lunch breaks.

My supervisor Jan-Leen, thank you for your sharp questions during our meetings, they gave me more insight in what I was doing and what I could improve in order to make things more clear and relevant. Danny, thank you for being part of my defence committee.

I would thank my family and my girlfriend for their never ending interest in my BEP, despite the fact that they really did not get what it was about most of the time. Thanks to Henko and Bertina for your comments on my draft version, which leads to an improvement of this thesis.

Lastly, I want to thank the whole NERA group, thanks for the sociability during lunch and coffee breaks, thanks for the delicious cakes and thanks to Jurriaan and Jan-Leen for the well-organized and very interesting excursion to Mol and Antwerp, which I really enjoyed.

CONTENTS

Chapter 1

INTRODUCTION

Since the resources of fossil fuels are limited, investigation in energy production is moving increasingly in the direction of the so called 'sustainable energy sources'. At this moment, the most important ones are: wind energy, solar energy, geological sources (steam and hot water) and nuclear energy (Dresselhaus & Thomas, 2001). Nuclear energy is a promising option and in the meantime there are loads of different reactor designs. One of them is the Light water reactor (LWR) where fuel rods are used to bring the fuel in the core and water is used both as coolant and moderator. At this moment the so called Generation IV reactors are the most innovative and safe reactor designs (Zhang, Wu, Wang, Xu, Sun, & Dong, 2009). Six different designs are being investigated in the Generation IV initiative. One of these is the Very High Temperature Reactor (VHTR) that makes use of helium gas coolant and graphite as a moderator. Several different designs are possible for this VHTR type reactor, one of them is the pebble bed reactor which will be the reactor design studied in this work.

1.1 PEBBLE BED REACTOR

1.1.1 DESIGN

One of the greatest differences between the pebble bed reactor (PBR) and a LWR is the method of refuelling. The PBR uses pebbles, with a 6 *cm* diameter, that are randomly stacked in the core with a packing fraction of 61% (Ougouag, A.M., Cogliati, & Kloosterman, 2005), instead of the fuel rods in the LWR design. These pebbles are made of graphite, which has two aims. Firstly, the rather obvious structural function; containing the fuel. Secondly, it acts as a moderator. Water is no longer needed as moderator, which makes it also possible to choose a gas coolant such as helium. The change of moderator in combination with the change of coolant allows for much higher temperatures then in water-moderated reactors. This temperature limit is now increased up to 750 °C, higher temperatures will gain structural damage for example on the metal elements of the core (Zhang, Wu, Wang, Xu, Sun, & Dong, 2009). The graphite pebbles are filled with smaller spherical so called TRISO particles, of about 0,5-0,7 mm that contain the actual fuel within three protective carbon layers. These TRISO layers will remain stable up to 1600 °C , this temperature is not

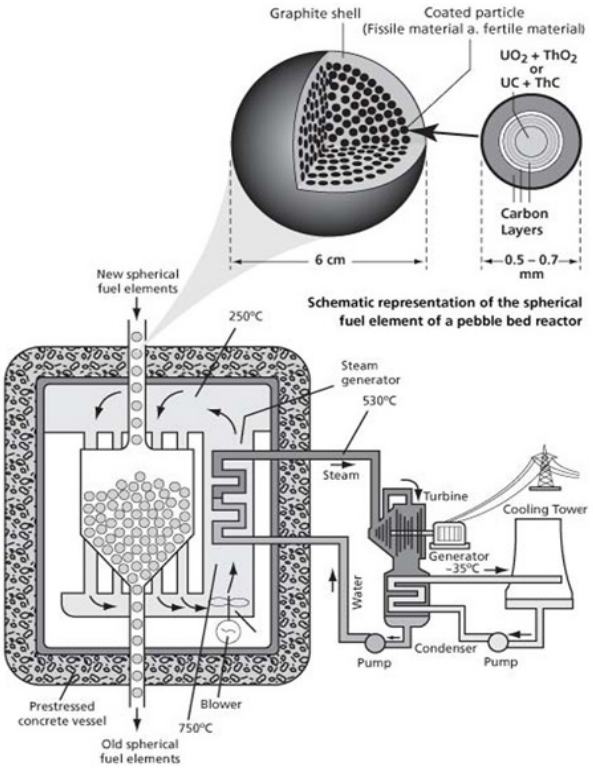

Figure 1.1: *Top: Fuel pebble design. Bottom: pebble bed reactor design.*

exceeded in case of an accident. There are more than 10000 of them in a single pebble (Zhang, Wu, Wang, Xu, Sun, & Dong, 2009). The pebble itself can be filled with up to 30 *g* of heavy metal (Wols, Kloosterman, & Lathouwers, 2012). A schematic view of a pebble and of a TRISO particle is given in the upper half of Figure 1.1.

The lower half of Figure 1.1 shows a schematic design of the entire pebble bed reactor. This type can be refuelled constantly, allowing for continues energy production (Zhang, Wu, Wang, Xu, Sun, & Dong, 2009). The pebbles are added at the top of the reactor vessel as well as the helium coolant, at 250 °C, which flows around the pebbles until it reaches the outflow at the bottom, at a temperature of 750 °C.

The pebbles are fed back several times, called pebble recycling. The multiple passing of the pebbles leads to a higher burn-up and less non-irradiated fuel in the waste. When the pebbles are finally removed out of the core it is possible to reuse parts of the waste again, in this work called actinide recycling, for only the highly radiotoxic minor actinides will be recycled in this work.

The helium coolant is blown upward by a blower to stream along a secondary water flow, where steam is generated. This secondary cooling system ensures that no radioactivity leaves the vessel in a different way than the outlet of the depleted pebbles. The cooled helium is fed back to the inlet at the top of the vessel, while the secondary stream of steam leaves the vessel through the concrete safety wall of the vessel. There it enters the power generating system, which consists of a turbine that drives a generator. Then it flows through a condenser after which it is pumped back in the steam generator as liquid water. In this survey the reactor core conditions are based on the specifications of the Chinese 2 x 250 MW_{th} HTR-PM demonstration plant (Zhang, Wu, Wang, Xu, Sun, & Dong, 2009).

1.1.2 SAFETY

Nuclear safety has been point of discussion for several decades, due to some nuclear accidents, from which Fukushima (WNA, 2014) and Chernobyl (WNA, 2014) are the most well-known. The PBR design has some safety advantages over the other reactor types. The decay heat can be removed passively due to the large surface-to-volume ratio at the core, while fuel temperature remain below 1600 °C. The maximum temperature for the TRISO layers won't be reached in this case, preventing leakage of nuclear waste out of the TRISO particles (Zhang, Wu, Wang, Xu, Sun, & Dong, 2009). One of the ways to shut down the reactor is with the use of control rods, similar to the conventional reactor designs. An inventive adjustment had to be made, the control rods wouldn't reach far enough in the pebble bed when inserted from top and bottom. Therefore the location changed to the graphite side reflectors, which makes that the control rods do not have to penetrate into the pebble bed anymore, due to the thinner core in the PBR design. The other inventive way to shutdown the reactor is with use of graphite control balls with neutron absorber material, such as boron. (Reutler & Lohnert, 1984)

The reactor is designed in such a way that the consequences of any conceivable incident would not lead to a significant release of radioactivity. The need of external intervention measures is eliminated also due to the passive cooling, e.g. conduction, radiation and natural convection can remove the decay heat also in case of failing of the active cooling system described earlier (Zheng, Shi, & Dong, 2009). Another safety improvement is the possibility to uncouple the primary and secondary cooling system thermohydraulically in case of failure, this prevents exposing the generator to extremely high temperatures. (Reutler & Lohnert, 1984)

1.2 THORIUM COMPARED TO URANIUM

Already in the 60's and 70's the problem of the limited uranium reserves was pointed out (Lung & Gremm, 1998). Unless the fact that 1 *g* of uranium, if completely fissioned, yields about 1 *MWd* of thermal energy (van Dam, van der Hagen, & Hoogenboom, 2005), it will be run out finally. However, this is quite a long time from now, there is a more important reason to search for a different fuel cycle, namely the production of minor actinides. Therefore research has been done on the thorium cycle instead of the uranium cycle. The conversion schemes of the thorium (Th-232/U-233) and uranium (U-235/U-238) fuel cycle look quite similar, as shown in Figure 1.2. However, the differences between the two fuels can lead to relevant differences in the radiotoxicity and decay heat production, since the mass number of Th-232 is lower than that of U-238.

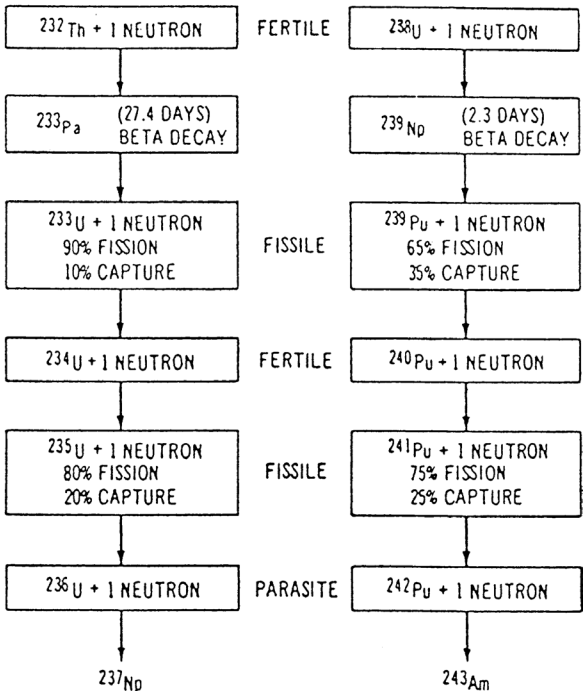

Figure 1.2: *Decay scheme of Th-232 (left) and U-238 (right)*

1.2.1 FUEL CYCLES

Uranium is available in the earth's crust with an average concentration of 2.8 ppm, while the earth crust contains 10 ppm Th-232 on average, which makes it 3 to 4 times more abundant than natural uranium. The mining of both thorium and uranium takes place mostly out of rocks and sand stones. Thorium is mainly mined as a by-product of monazite sand (IAEA, 2005). The extraction of the thorium takes place using a nitric acid solution. This leads to the desired ThO_2 which can be used in the fuel pebbles.

As Figure 1.2 shows U-238 itself is not a fissile isotope. First Pu-239 is generated by neutron capture and two subsequent beta decays. This Pu-239 is fissile. It has a capture to fission ratio of about 0.5 (Hopkins & Diven, 1962) which means that about one third of the neutrons will not contribute to the energy production but produces long-lived actinides. In order to achieve a critical reactor the fraction of fissile U-235 is increased in the fuel, by enrichment.

In the thorium fuel cycle, fissile U-233 is produced by neutron capture in Th-232 followed by two beta decays. The capture to fission ratio of U-233 is about 0.11 (Hopkins & Diven, 1962) so the probability of building up heavy actinides is considerably lower than for Pu-239 in the case of uranium fuel. Furthermore, U-233 should undergo a few additional neutron capture steps before it is at the level of Pu-239. To achieve criticality U-233 is added as a driver fuel. However, U-233 does not occur in nature so it has to be produced in an external cycle or U-235 or Pu-239 has to be added to create a critical reactor design. (NNL, 2012)

1.2.3 THEORETICAL COMPARISON

The first difference between the two fuel cycles arises immediately at the moment of mining. The total radioactive waste production for the uranium fuel during the mining is about two times higher than for the thorium fuel. Thereby also the radon effect (Rn-222), that occurs in the uranium fuel case is much greater than the equivalent thoron (Rn-220) effect in the thorium case. This makes it a bit easier and safer to deal with, because the workers will be exposed to a lower dose. (WNA, 2012)

The thorium fuel cycle leads to less minor actinides than the uranium fuel cycle in thermal reactors such as the pebble bed reactor, because of the lower capture to fission ratio of U-233. However, when the design of a fast reactor is used, this advantage of thorium disappears. Since the number of neutrons produced per absorbed thermal neutron is higher than two for U-233, thorium can also be used for breeding (IAEA, 2005). The potential for breeding in a thorium fuelled pebble bed reactor was investigated by Wols (Wols, Kloosterman, & Lathouwers, 2012).

Another advantage at Th-232 in a PBR is the intrinsic proliferation-resistance of Th-232. During the burn-up and decay of thorium pebbles U-232 is formed, which has a half-life of only 73.6 years and some of its daughter products with also short half-life are strong gamma emitters. This creates a barrier against proliferation e.g. production of nuclear weapons. On the other hand, it makes it harder to handle the nuclear waste and to reprocess the fuel. (Lung & Gremm, 1998)

1.3 RADIOTOXICITY

The most interesting subject in dealing with nuclear energy production, with respect to this thesis work, is the ionizing radiation emitted by the nuclear waste and its potentially harmful biological effects. In the worst case a very high dose can lead to immediate death but it is already an issue when humans are being exposed to a smaller dose. The quantity that specifies this phenomenon in equivalent dose is the radiotoxicity in Sieverts *[Sv]*. The equivalent dose is a measure for the amount of radiation to which a specific tissue is exposed. The dependence on different radiation types and parts of the human body are tried to be implemented in this equivalent dose. See the theory chapter for a more extensive description of equivalent dose (radiotoxicity). (Bos, Draaisma, & Okx, 2007)

The radiotoxicity, or in fact the activity, has its roots in the instability of certain nuclei. A nucleus consists of positively charged protons and neutral neutrons. The strong nuclear force, the repulsive force between the protons and neutrons, induces stability inside the nucleus. However, a nucleus can be unstable if the ratio between protons and neutrons is unfavourable (this means that it has a limited lifetime). Such nuclei have an energy surplus while they desire to be in the stable situation with the lowest energy. This surplus of energy is released as ionizing radiation during decay at the nucleus. (Bos, Draaisma, & Okx, 2007)

The radiation is subdivided in a few different categories; α, β and γ radiation are the most common ones. In the theory chapter these different radiation types will be specified and discussed more extensively.

The activity is defined as the number of spontaneous decays per unit time, and has the unit Bequerel *[Bq]*, after its discoverer. So 1 *Bq* is 1 decay per second. However, it is impractical to define radiation limits in terms of activity because of the different radiation types and their specific influence on specific parts of the human body. Radiotoxicity enables this via conversion coefficients that are defined by the International Commission on Radiological Protection, ICRP, for both inhalation and ingestion of specific radioactive isotopes. In this work, the coefficients for ingestion are used to transfer the activity to radiotoxicity for ingestion seems to be the most realistic scenario. Appendix C contains these coefficients which are according to ICRP Technical Report Publication 68. (ICRP, 1994)

1.4 DECAY HEAT PRODUCTION AND STORAGE

Radiation emitted by an instable nucleus, i.e. radiotoxicity, has been discussed already, but the energy in the form of radiation leads to a second problem: the conversion of radiation to heat. The nuclear waste has to be stored for a very long time up to million years, until it is no longer harmful to human health. During this storage the unstable nuclei have to decay to stable ones under emission of radiation which is converted in heat. This decay heat production is the biggest limitation to deal with the initial storage of nuclear waste. Since, when the pebbles are irradiated and no longer reprocessed they have to be stored somewhere. In order to reduce the potential high temperatures of the nuclear waste it has to be stored for about 100 years, the decay time of fission products to their stable daughters, in a short term storage before it can be stored definitively. Most of the nuclear power plants have their own short term storage basin. (NRC, 2002)

However, if the capacity of the wet storage is reached, the waste has to be stored dry; above the ground. The spent fuel goes into a container, filled with inert gas, called a cask. They are made of concrete and metal. Dry storage is only possible after the waste has been cooled down to a certain level by storage in a storage pool for several years. (NRC, 2002)

After heat production has dropped below a suitable level, the waste has to be moved to a long term storage place, because of the fact that it remains radiotoxic for almost a million years. These long term storages have to satisfy at least two requirements: It must protect the environment from radiation during the whole storage time and no structural damage may occur due to the decay heat produced. The best option for long term nuclear waste storage seems to be underground. Suited ground layers are, salt, clay and tuff, a volcanic material (ESV Euridice EIG, 2010). For instance, the Yucca Mountain project in Nevada would be a suitable storage place for the American nuclear waste. Studies and surveys has been done on the composition of the volcanic material, where it's made of, in order to determine whether or not Yucca Mountain would be suitable for long term storage. Definitive results or advanced plans are still not there, partly due to the stop on the funding of the American government since the reign of Obama (Garvey, 2012). Also in Europe research and development is done on a possibility for long term storage, because not everywhere the same ground layers are available. For instance Boom Clay, located in the northern part of Belgium, provides an interesting ground layer to store long term nuclear waste.

1.5 ACTINIDE RECYCLING

To lower the amount of radiotoxicity or decay heat per unit energy produced it is an interesting option to recycle some useful minor actinides of the depleted pebble. This is possible because not all fuel will be consumed during irradiation while also some new useful isotopes are produced. When certain highly radioactive actinides are added in the recycled pebble, the total amount of radiotoxicity and decay heat per unit energy can be reduced, because these actinides can become fissile or transform into a less radiotoxic isotope after neutron capture.

However, it is rather difficult to break up the pebble and the TRISO particles contained so that the different elements can be separated and re-used. In the most promising method, pebbles are poured into a vessel filled with water. An electric shock is produced in the water, which causes a subdivision of the pebble into its TRISO particles and graphite pieces. A second shock is produced in order to remove the outer layers of the TRISO particles. This method is also energetically justified, because it consumes only 0.125 to 0.25 percent of the electricity output before actinide recycling. (Fütterer, von der Weid, & Klichmann, 2010)

However, this method is only demonstrated in a lab environment so far, so further development is required for large scale application or other pebble splitting methods have to be considered in order to make recycling of the burned-up pebbles possible. However, assuming that it will be possible to break up the pebbles, a few recycling strategies will be considered in this thesis.

For this thesis work, recycling the fuel of the pebble bed reactor separates only a few actinides while the other part of the spent fuel is stored in a short term storage until the recycling has taken place. Than the total of actinides and fission products is moved to the long term storage, as it happened also in the case without actinide recycling.

To obtain a closed fuel cycle it is important that the starting concentrations of the fuel are the same for every recycling step, namely the starting configurations of the first step. This can be managed in several ways. Considering the case of the Th-232/U-233 case, in the starting condition the pebble contains a fraction p U-233 and a fraction (1-p) Th-232 and a two times this amount of oxygen, because the fuel is entered in form of ThO_2 and UO_2 (Wols, Kloosterman, & Lathouwers, 2012). Finally the TRISO layers and cladding material of the pebble have to be added every burn-up step, which will only effect the cross section calculations due to their specific influences on the neutrons.

Three recycling strategies are investigated in this work. Firstly. the thorium non-critical breeder configuration. The desired closed U-233 cycle can be reached, however criticality would not be obtained due to a shortage of neutrons on the nuclide balance. The second method tries to overcome this problem by adding a larger fraction of U-233 each recycling step. However, this U-233 has to be produced somewhere external for instance with the use of an accelerator driven system, ADS. (Vandeplassche, Biarotte, Podlech, & Klein, 2011) The third method is based on adding a certain fraction of reactor grade plutonium which will be added instead of the additional U-233. With the same goal, overcoming the shortage on the neutron balance and thus criticality. These three methods will be discussed more extensively in the models chapter.

1.6 AIM OF THIS WORK

The aim of this work is to investigate the differences in radiotoxicity and decay heat production between an uranium and a thorium fuelled pebble bed reactor. It is expected that the thorium fuel cycle leads to a lower total radiotoxicity during decay. Another interesting question is whether a similar reduction in heat production occurs.

A second question that rises is related to actinide recycling. How beneficial is the recycling some highly radiotoxic actinides with respect to storage, in terms of the radiotoxicity, as well as the decay heat? Could this lead to a significant decrease in radiotoxicity and decay heat production per unit energy? It seems plausible to think so, because of the reduced formation of radiotoxic higher actinides. Several repetitions of recycling will be compared in order to see if some equilibrium can be reached.

Chapter 2

THEORY

2.1 NUCLIDE BALANCE EQUATIONS

The burn-up calculations done during this survey make use of a nuclide balance equation, in which the different production and loss terms of nuclide X are present. A basic form of the nuclide balance can be given by Formula (2.1)

$$\frac{dN_X}{dt} = \text{Formation Rate - Destruction Rate} \pm \text{Decay Rate} \tag{2.1}$$

Here N_x is the contribution of nuclide x. The formation rate can be subdivided in formation due to neutron capture or by fission of a different nuclide. While the destruction rate consists of neutron absorption by nuclide X, which comprises both fission and capture. The decay term could work in both directions. Formula (2.2) gives the total nuclide balance of nuclide X (Massimo, 1976)

$$\frac{dN_X}{dt} = \phi \sum_i N_i \sigma_{f,i} y_{i,X} + \sum_j N_j \sigma_{c,j} \gamma_{j,X} + \sum_k N_k \lambda_k \alpha_{k,X} - \phi N_X \sigma_{a,X} - \lambda_X N_X \tag{2.2}$$

Where $N_n =$ atomic concentration of isotope n,

$\sigma_{c,n} =$ capture cross-section of isotope n,

$\sigma_{f,n} =$ fission cross-section of isotope n,

$y_{i,x} =$ yield of isotope X due to a fission in isotope i,

$\gamma_{j,x} =$ probability that a neutron absorption in isotope j produces isotope X,

$\alpha_{k,X} =$ probability that the decay of isotope k produces isotope x,

$\lambda_n =$ decay constant isotope n,

$\phi =$ flux.

The first term on the right-hand side of the equal sign gives the loss of nuclide X due to absorption, the following two terms give the contribution due to fission and neutron capture by different nuclides respectively. The last two terms signify the changes in nuclide concentration due to decay.

In this work a constant power was chosen, which makes it possible to calculate the flux as function of time with use of Formula (2.3). (Gauld, Hermann, & Westfall, 2009)

$$\phi(t) = \frac{P}{e \sum_i N_i(t) \sigma_{a,i} Q_{a,i}} \tag{2.3}$$

Where P = Power Density $[MW/cm^3]$

N_i = the number of atoms for nuclide i

$\sigma_{a,i}$ = the reaction absorption cross-section for nuclide i, [cm^2](absorption = fission + capture)

Q_i = the recoverable energy in [MeV] released from fission and capture

$e = 1.6 \cdot 10^{-19}$ [J/eV], joule to electron volt conversion factor.

All these quantities are given as input to the ORIGEN-S code used in this work in order to calculate the burn-up of the reactor. The specific power and number of atoms are adjusted and given as input variables. The cross-sections are calculated and updated with use of programs called CSAS and Couple, which will be discussed in more detail in the models chapter (Gauld, Hermann, & Westfall, 2009).

2.2 ACTIVITY, RADIOTOXICITY AND DECAY HEAT

Nuclear radiation is subdivided in a few different categories; α, β and γ radiation are the most common ones, see Figure 2.1. In case of α-radiation a helium nucleus is emitted and the mass number of the initial nucleus decreases with four while the number of protons decreases with two. The helium nucleus has an energy between 4 and 8 MeV. It will be higher for initial nuclei with a shorter half-life and the other way around. (Bos, Draaisma, & Okx, 2007)

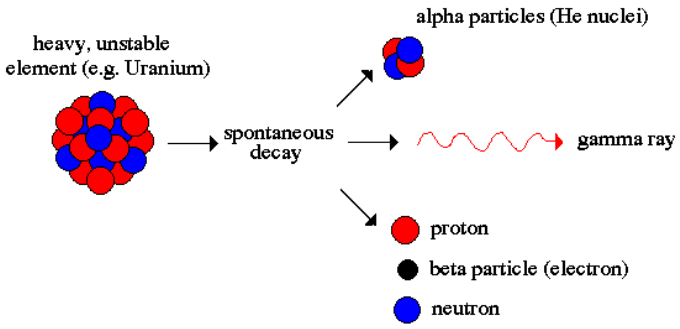

Figure 2.1: *Schematic of an unstable nucleus with its different possible decay effects.*

β radiation is divided in two types; β^- and β^+ radiation. β^- decay takes place if the specific nucleus has a neutron excess. To reduce the surplus of neutrons one neutron is transformed into a proton under emission of an electron and an anti-neutrino. The mass numbers of the initial (mother) and final (daughter) nuclide are the same since a neutron was changed into a proton. The total energy of the irradiated particles is of the order of a few MeV's. The second form of β radiation is the β^+ decay which can be emitted in case of proton excess. One proton is converted into a neutron, while a positron and a neutrino are emitted with a total energy of about 1 MeV. (Bos, Draaisma, & Okx, 2007)

The last category is γ radiation, which occurs usually after an α or β decay. The daughter product will be in an excited state and will move to an state with lower energy by emitting γ radiation. The energy of the emitted photons lays somewhere between a few hundred keV and 10 MeV. (Bos, Draaisma, & Okx, 2007)

Activity is the important quantity in defining the radiotoxicity of a certain nuclide. It indicates the rate at which nuclide change takes place, see Formula (2.4).

$$A = -\frac{dN}{dt} \tag{2.4}$$

Activity is directly proportional to the number of present radioactive atoms:

$$A = \lambda N \tag{2.5}$$

Where λ [s^{-1}] is a specific radionuclide dependent decay constant. Filling in this expression in Formula (2.4) leads to the following differential equation

$$\frac{dN}{dt} = -\lambda N\,, \tag{2.6}$$

which has the following solution:

$$N(t) = N(0)e^{-\lambda t} \tag{2.7}$$

Where $N(t)$ and $N(0)$ are the number of atoms of a specific radionuclide available at a time t and at time 0 respectively. Because of the directly proportionality of the activity and number of atoms, see Formula (2.5), the activity is an exponential function of time:

$$A(t) = A(0)e^{-\lambda t} \tag{2.8}$$

Where $A(t)$ and $A(0)$ are the activities at time t and time 0 respectively.

One of the characteristics of an exponential function is that in equal time steps, equal fractions will disappear. Taking this into account, it is more convenient to make use of the half-life, defined as:

$$T_{1/2} = \frac{\ln(2)}{\lambda} \tag{2.9}$$

Filling in this half-life in Formula (2.8) gives the law of decay in terms of the half-life. The half-life is a well-known quantity that is provided for each isotope for instance on a table of nuclides.

$$A(t) = A(0)\left(\frac{1}{2}\right)^{\frac{t}{T_{1/2}}} \tag{2.10}$$

As mentioned before in the introduction, radiotoxicity is a much more useful quantity to use, for this also takes into account the influence of the different types of radiation, upon the different parts of the body irradiated. This makes it possible to compare the contribution of all kind of isotopes. Formula (2.11) shows the relation between activity and radiotoxicity.

$$T = A \cdot DCN_{\text{ICRP 1994}} \tag{2.11}$$

Where T = Radiotoxicity in [Sv]
A = Activity [Bq]
$DCN_{\text{ICRP 1994}}$ = Dose coefficients of nuclides for ingestion as in ICRP Publication 68 (1994) [SvBq^{-1}]

The decay heat production calculations in ORIGEN-S are directly linked to the activity data. With use of a multiplication factor, which takes into account the specific contribution of the different nuclides. This coefficient acts in the same way as the $DCN_{\text{ICRP 1994}}$ in Formula (2.11)

All these formulas are used in the models described in the next paragraph. (Bos, Draaisma, & Okx, 2007)

Chapter 3

MODELS

To move from the theory, discussed previously, to the results part following this chapter, some computational models are used to calculate burn-up, k_{inf}, radiotoxicity and decay heat production data. This data can be used for comparisons of several simulation cases and to make summarizing graphs. The main modules used in this survey, as given below, will be mentioned and discussed in this chapter:

- Cross section generation and Burn-up and calculation – '*Burn_up_loop'*
- Radiotoxicity and Decay heat production calculations – *'Decay_loop'*
- Actinide recycling

The first model will be discussed briefly and only the basics will be mentioned. For further insights in this model one can have a look into Wols, Kloosterman & Lathouwers (2012). The model used in this survey is based on the '*Burn_up_loop'* model which is written by Wols and briefly explained in this chapter.

The second model will be discussed in more detail, because this was specifically generated and implemented for this study. Before the discussion of this model a block scheme will be given to give an overview and a brief explanation of the code written, which is called *Decay_loop*.

The recycling model is basically based on the two previous models with some merging additions. The aim of these additions will be discussed as well as their implementation.

3.1 CROSS SECTION GENERATION AND BURN-UP CALCULATIONS – '*BURN_UP_LOOP*'

The starting point of all the simulations and calculations done in this survey is the code written by Wols, named '*Burn_up_loop*' (Wols, Kloosterman, & Lathouwers, 2012). This code consists of several parts and modules of the SCALE6 code package (ORNL, 2009), one of them is ORIGEN-S. A schematic model of this code is given in Figure 3.1.

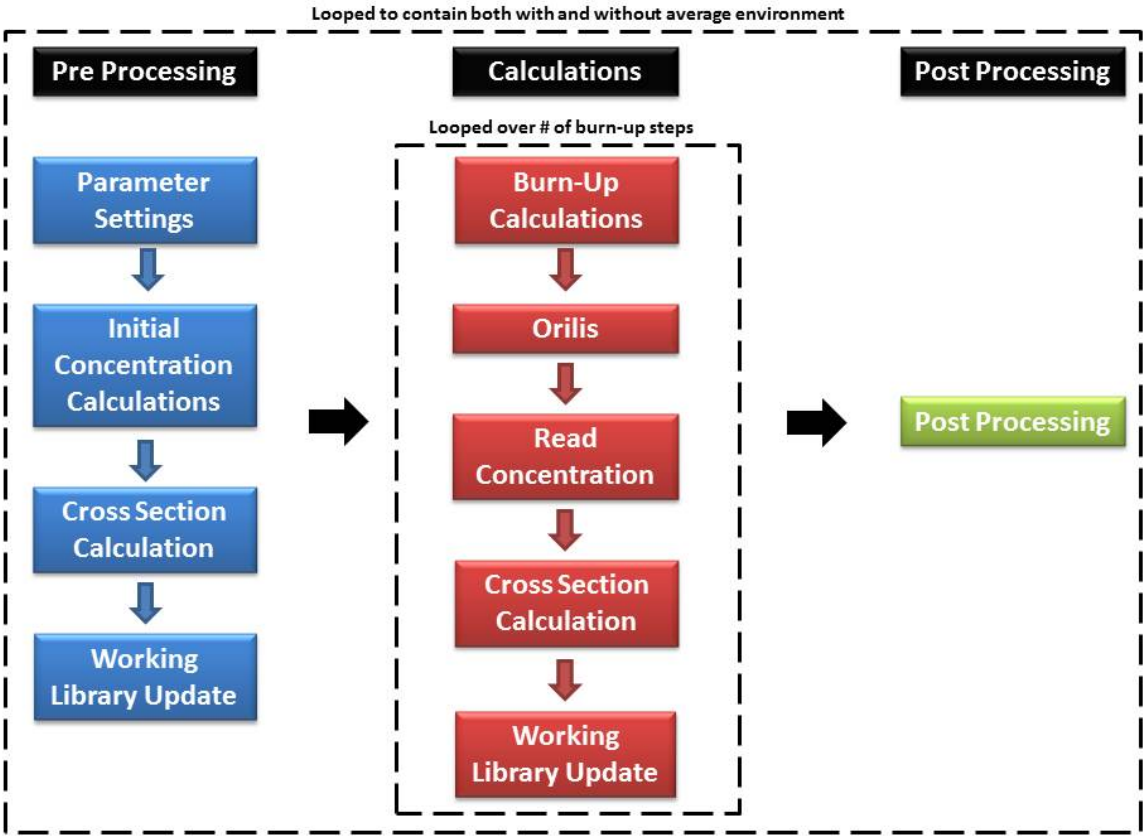

Figure 3.1: *Schematic model of the code 'Burn_up_loop'.*

The code consists roughly of 3 parts; pre-processing, calculations and post processing. In the pre-processing phase the variable parameters has to be stated in *'parameter settings'* and *'initial concentration calculations'*.

The '*Burn_up_loop*' has two main objectives. First, to calculate the cross sections, the required geometric parameters of a single pebble are defined by the user in the parameter settings. After the calculation of the cross sections the second objective of the code comes into play, the calculations of the burn-up. For these the cross sections are required, because the burn-up depends on the interaction of the pebble with the available neutrons, see chapter 2. The cross sections give insight in the ability for neutrons to interact. Also a constant power and a constant heavy metal loading of the pebble are needed to get the desired output in units of GWd/th. Lastly, in the *'Initial Concentration Calculations'* the initial concentrations and a list of isotope identifiers is set, namely these from the ENDF-V5 238 group (ORNL, 2009). These are necessary to couple the calculated concentrations to the right isotope, to make it possible to post process them. After these parameter settings and initial concentration calculations the first cross section calculation takes place and the ORIGEN working library is updated to account for the proper neutron spectrum.

Then the burn-up calculation phase begins. As mentioned in the figure, this part cycles trough the number of burn-up steps, which has been specified in the pre-processing part. Each loop starts with the actual calculations of the burn-up. The relevant data, i.e. the mass concentrations and the k_{inf}, is saved. Therefore the '*Orilis*' code is called. This program extracts the data from the binary files provided by the ORIGEN depletion calculations. Using the extracted data, an update of the cross sections and working library can be made and after that the loop will move to the next burn-up step.

When all burn-up steps are done, the post processing phase starts. The aim of this phase is to store all the interesting output data in a MATLAB output format. This makes it easier to produce the graphs and analyses in the result chapter.

After this, the whole burn-up calculation is done, however as mentioned in the picture this total of pre-processing, calculations and post processing is looped so that both without and with average environment of the single pebble are simulated. This requires some explanation, the burn-up calculation without the average environment is a depletion calculation on a single pebble. The only included external effect is the reflective boundary condition. This makes the calculations much easier and faster, however, to make it more realistic the environmental effects of the pebble have to be added. This is done in the second part of the loop, 'with average environment'. The idea is that the single pebble of the ORIGEN depletion calculation for one pebble is put in an environment that satisfies the conditions of an average pebble, which can be extracted from the 'without average environment' case. Resulting in a more realistic multiple pebble model, in order to simulate a real pebble bed. See Figure 3.2 for a schematic design of this model.

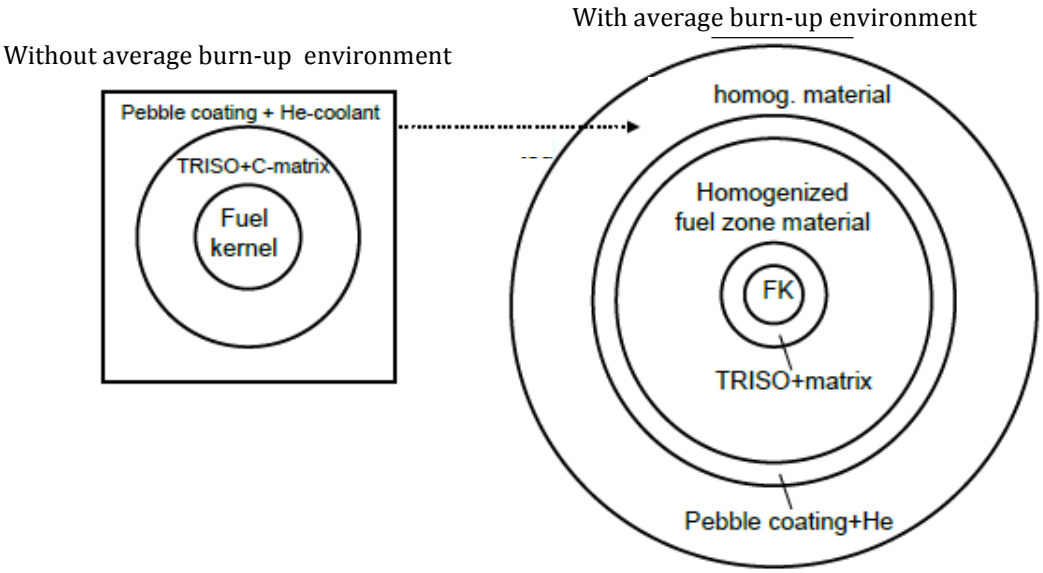

Figure 3.2: *Schematic model of the case without (left) and the case with (right) average environment as it is implemented in the burn-up code.*

© Wols

So, the first loop calculates the whole burn-up for just a single pebble. The second loop uses the output of this loop to calculate the whole burn-up again, but now with the average environment based on the conditions of an average pebble. This second loop provides the data which can be used for further calculations. The use of a single pebble is not realistic, but the addition of the average burn-up environment makes the simulations more accurate. As mentioned before this code was written by Wols, however the code has been adjusted at several places to make it appropriate for this survey.

3.2 RADIOTOXICITY AND DECAY HEAT PRODUCTION CALCULATIONS – *'DECAY_LOOP'*

The codes used for this part of the calculations were written and adjusted for this specific survey (by the author of this thesis). The main code, '*Decay_loop'*, consist of several small scripts that will be discussed in this paragraph. The code written is mostly based on the previously discussed '*Burn_up_loop'* and thus on the SCALE6 package, including ORIGEN-S. However some specific modifications were made to make it possible to extract the right data. Before discussing this model, a schematic overview of the '*Decay_loop'* script is given in Figure 3.3.

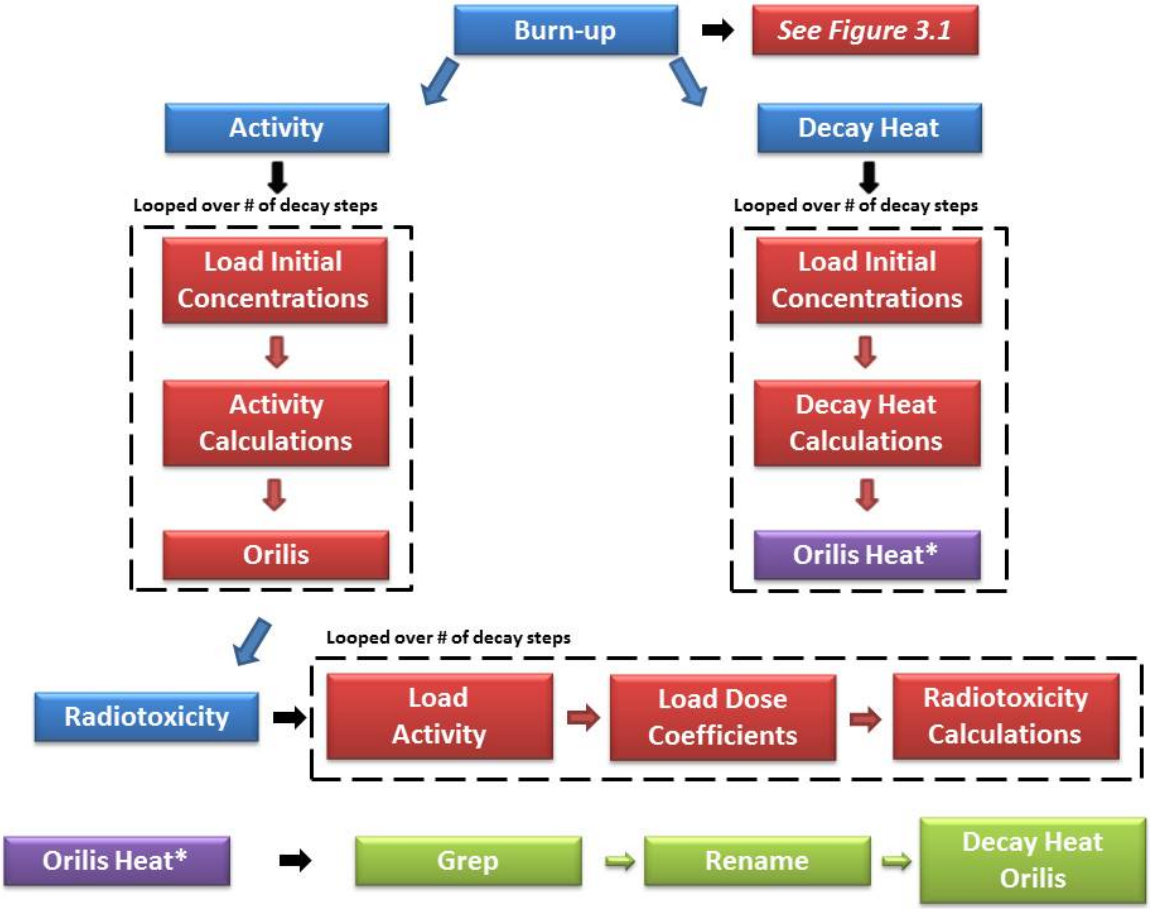

Figure 3.3: *Schematic model of the code 'Decay_loop'*

The main '*Decay_loop'* script starts with some parameter settings, namely those earlier discussed for the '*Burn_up_loop',* the total decay time and the intervals between each decay step. In this work a rather long decay time has to be taken in account. The period of the first 100 years gives some insight in the decay of most of the fission products, while an analysis of the actinides requires a huge timescale of about 1 million year. It is unnecessary to simulate the data with time steps of a single year at this huge timescale of 1 million year, while this is desirable on short term, e.g. the first 10 years. For this reason a kind of logarithmic scale is applied in the decay steps. Table 3.1 gives an overview of the intervals used in this work and it makes clear that only 55 steps are needed to reach the time scale of 1 million years. This logarithmic time scale assumption was compared to a simulation with equal time steps of 1 year each and they were equal up to 0.002 percent, this makes it an appropriate application.

Table 3.1: *Logarithmic scale on time intervals in the decay loop. The first row contains 10 steps, which count each for 1 year. The second row contains 9 steps, namely the time intervals from 20 years till 100 years. The third row contains 9 steps as well, but with a time difference of 100 years between each decay step and so on until the last row, with a time difference of 100000 year between each decay step.*

Interval size *[year]*										**Total # of steps**
1	2	3	4	5	6	7	8	9	10	**10**
	20	30	40	50	60	70	80	90	100	**19**
	200	300	400	500	600	700	800	900	1000	**28**
	2000	3000	4000	5000	6000	7000	8000	9000	10000	**37**
	20000	30000	40000	50000	60000	70000	80000	90000	100000	**46**
	200000	300000	400000	500000	600000	700000	800000	900000	1000000	**55**

The first script called in the *'Decay_Loop´* is the *'Burn_up_loop'* exactly as it was described in paragraph 3.1. Thereafter the calculation of the activity takes place, this starts with the loading of the initial concentrations after depletion from which the activity will be calculated. These are the ones provided by the last burn-up step for the case with average burn-up environment of the *'burn_up_loop'*. This is rather obvious as from here the nuclear waste has to be stored and the decay starts. Thereafter the actual activity calculations are done, using the ORIGEN-S package of SCALE6. The settings are almost the same as in the *'burn_up_loop'*, except the output that is printed. In this case the activity has to be extracted instead of the concentrations after burn-up. Another different setting is the desired power, obviously this is set to zero in the decay calculations, because there is no irradiation. The last step is again the *'orilis'* code that extracts the activity data from the binary output file for analyse in MATLAB. The whole activity phase is looped for the total number of decay steps, so 55 times in this survey.

The third step in the *'Decay_loop'* code is the conversion from activity [*Bq]* to radiotoxicity [*Sv]*. This part starts with reloading the calculated activities from the previous step. These activities are multiplied with the corresponding dose coefficients of the nuclides, as mentioned in the theory chapter. The dose coefficients for ingestion are used, as it is more likely to ingest nuclides of the waste than to inhale them in this situation of storage. These dose coefficients are given in ICRP's Technical Report Publication 68 (ICRP, 1994), and shown in Table C.1 of appendix C. Some nuclides formed in the burn-up phase are not provided in this publication, probably because their contribution to the radiotoxicity is negligible or they are unknown. Furthermore the mass concentration of these few isotopes is extremely low in comparison with the others, so these isotopes won't be taken into account. After the multiplication with these dose coefficients [*Sv/Bq*] the radiotoxicity [*Sv*] is saved also in a MATLAB readable format. Of course, the whole radiotoxicity phase will also be looped for the amount of decay steps.

The final script of the *'Decay_loop'* code calculates the heat production. This phase is almost the same as the activity phase. Also this script starts with loading the initial concentrations provided in the last step of the case with average burn-up environment of the *'Burn_up_loop'*. The only difference between the calculation of the activity and the decay heat is one setting in the ORIGEN-S code, in order to print the decay heat production [*W*] instead of the activity [*Bq]*. The remainder of the script is the same as for the activity calculations. However, there is a slight problem in the data processing, because the '*Orilis'* script cannot extract the decay heat out of the binary file. To resolve this problem a specific program is written, as mentioned in the bottom line of Figure 3.3. The first element of this program is the *grep-command* which is used to select the decay heat data from the generated output file. The next program *'Rename'* renames the output of the *grep-command* and gives it a *txt* extension, which is needed as input of the final script, *'Decay_Heat_Orilis*' that returns the final MATLAB readable output. Also this decay heat phase has to be looped for the total number of decay steps.

3.3 ACTINIDE RECYCLING

Several adjustments and additions were made to the code schemes discussed in paragraph 3.1 and 3.2 in order to model the effect of actinide recycling on the radiotoxicity and decay heat production of the waste. Figure 3.4 gives a schematic overview of the code used to include recycling.

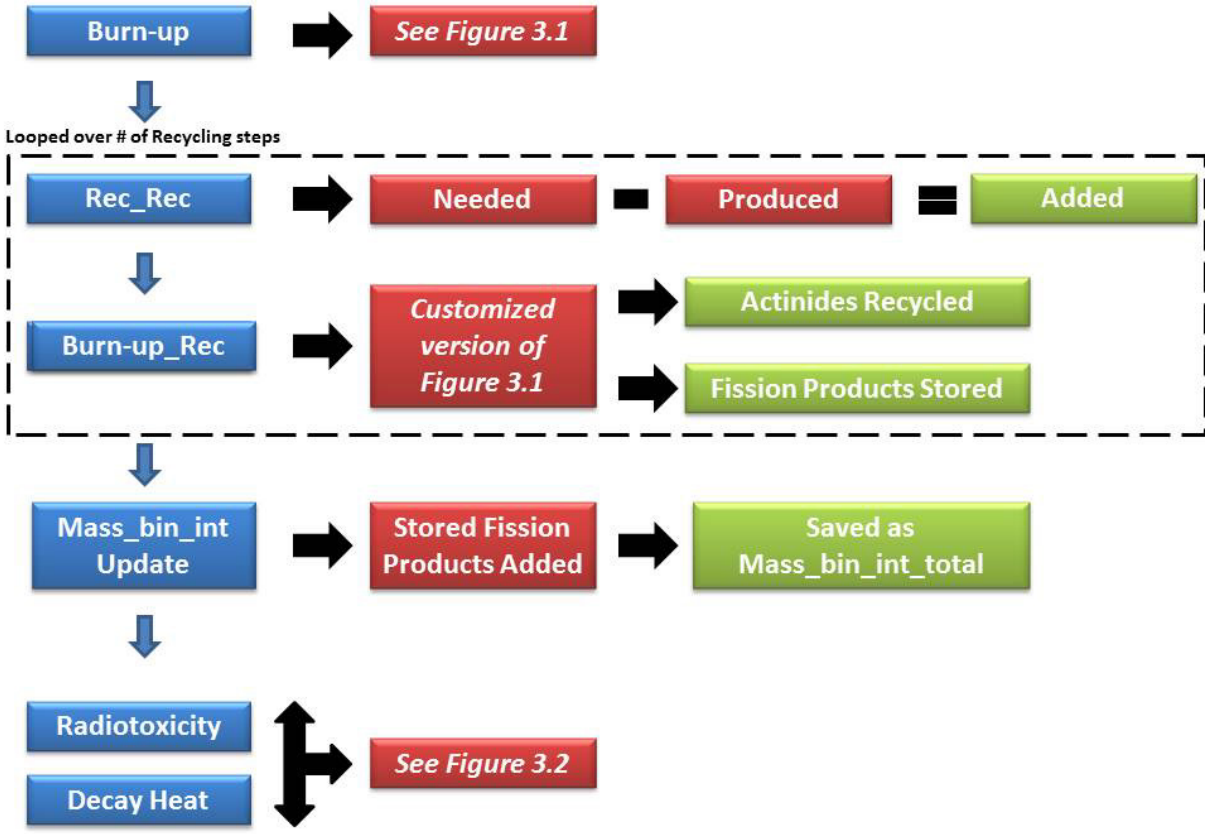

Figure 3.4: *Schematic model of the code used for the recycling simulations*

The whole code starts with the main file that links all the boxes in blue. All the important parameters, such as number of irradiation steps, number of recycling steps, decay time, enrichment, etc. can be set in this file. There is also the possibility to choose for a simulation with or without recycling. After these settings are adjusted, the actual simulation starts with the first cross section and burn-up calculations as described already in paragraph 3.1. The output concentration vector is used as input for the next program, *Rec_Rec*. The aim of this program is to check the amount of thorium, uranium and/or plutonium that have to be added in order to get the same concentrations as the initial fuel concentration.. The calculated addition of thorium, uranium, which will be 0 in the recycling configurations, and plutonium are saved. At the moment this is done, the composing of the fuel can take place in both recycling strategies. The fission products produced in the first burn-up will be removed and stored for the time the total recycling will take. After updating the fuel composition, the first recycling step can be done, this consists of a cross section calculation followed by a burn-up calculation similar to the once through model. The concentrations of all the isotopes will act as input for the *Rec_Rec-script*, where this loop started. This loop continues until the number of recycling has been reached. At this point, the total waste concentration vector is determined after addition of the stored fission products of each step. This total waste concentration vector will be the input of the radiotoxicity and decay heat calculations already described in paragraph 3.2.

As mentioned already in the introduction chapter, three types of recycling were considered in this work. The following paragraphs discuss their possibilities, assumptions and drawbacks.

3.5.1 THORIUM NON-CRITICAL BREEDER CONFIGURATION

The first option is a net-breeding option. This means that the starting pebble is configured in such a way that the output U-233 concentration after burn-up is the same as the input concentration. The great advantage of this method is the possibility to keep the reactor in operation without additional fuel except thorium, in the form of ThO_2. However, it is impossible to reach criticality for this single pebble configuration. The k_{inf} will stay below 1, which means that the neutron balance is no longer right (van Dam, van der Hagen, & Hoogenboom, 2005). This means that this option is not suitable enough to deal with the required starting conditions.

3.5.2 URANIUM PRODUCTION WITH USE OF A LINAC

A second option is to start with a certain enrichment of a few percent of U-233, but higher than the amount produced after irradiation. The additional fuel required to reach criticality needs to be produced somewhere else, as it is not produced from the thorium in the core. Additional U-233 can be produced for example by neutron capture of Th-232 in another reactor, due to the shortage of neutrons in the PBR core. The required neutrons for the external U-233 cycle can also be produced by a Linac such as the one of the Myrrha project in Mol (B). This is a linear accelerator, which accelerates protons up to 600 MeV, after which they hit a target. Due to this collision a certain amount of neutrons is produced, up to 15 per 600 MeV proton (Vandeplassche, Biarotte, Podlech, & Klein, 2011). In an ideal world, all these neutrons can be used to produce U-233. Of course, the thorium fuel has to be supplemented with fresh ThO_2 each recycling step until the required starting conditions are reached.

The great advantage is that criticality can be reached in the pebble bed reactor, since this was not possible for the previous option. However, the greatest problem is the energy use of the linear accelerator itself. A best case scenario calculation of this possibility is done in appendix A and shows that this option is energetically not beneficial, so another option has to be investigated. However, further research can be done on the influence of fission by fast neutrons in the ADS upon the energy efficiency, which is only possible when the assumption of sole neutron capture by U-233 is no longer made.

3.5.3 PLUTONIUM CLOSED URANIUM CYCLE ADDITION

The final possibility to get a suitable starting and recycling configuration is to add reactor grade plutonium (Sahin, Sahin, & Acir, 2012) to the fuel to reach a critical core configurations. Some plutonium isotopes are fissile and takes over a part of the task of U-233. This leads to the starting fuel composition in Table 3.2 for each recycling step as well as the first burn-up cycle.

Table 3.2: *Fuel composition of the Plutonium closed Uranium cycle case.*

Fuel composition	Share
U-233	pU %
Reactor Grade Plutonium	pPu %
- Pu-238	*1% at pPu %*
- Pu-239	*62% at pPu %*
- Pu-240	*24% at pPu %*
- Pu-241	*8% at pPu %*
- Pu-242	*5% at pPu %*
Th-232	(1 – pU –pPu) %

The idea is to start with a certain amount of Th-232, U-233 and reactor grade plutonium in such a way that exactly that amount of U-233, needed each burn-up step, is produced. This means no additional U-233 is required in a new recycling step. Only the ThO_2 and the reactor grade plutonium have to be added, the last can be imported from other reactors, which have no use for it. (Sahin, Sahin, & Acir, 2012) The closed U-233/Pu cycle has two advantages, the produced U-233 during every single burn-up cycle can be reprocessed, so this reduces the nuclear waste and no extra U-233 has to be produced somewhere else.

Chapter 4

RESULTS

This part of the thesis is divided in a part without and a part with actinide recycling. Firstly, a complete overview of the case of a single pebble without recycling is given. Secondly, the actinide recycling case will be analysed. In the first configurations a comparison will be made between the case with U-235/U-238 (Zhang et al, 2009) and the one with Th-232/U-233 as fuels. In the actinide recycling case a comparison will be made between the Th-232/U-233 case and the different recycling methods described in the method section. It was also mentioned already that the main comparisons are performed on the radiotoxicity and heat production. Also the contributions of the different fission products and actinides are examined. All simulations are done using the *Decay_loop* program, which has been written and updated for this Bachelor thesis (see the models chapter).

The reactor core design of a pebble bed reactor was already shown in paragraph 1.1. A typical core contains around 300,000-500,000 pebbles (Zhang, Wu, Wang, Xu, Sun, & Dong, 2009). However, this is rather difficult to deal with in first calculation, for this reason some simplifications have been made. The most simplified reactor core model is that of a single pebble, which contains all the fuel available in the kernel, instead of the total of randomly stacked pebbles containing each a part of this total fuel. This makes it relatively easy to handle and to deal with. This single pebble model is used in all the simulations in this survey. In further surveys it may be interesting to focus on a more realistic core model.

4.1 SINGLE PEBBLE – WITHOUT ACTINIDE RECYCLING SIMULATIONS

4.1.1 PARAMETER PREPARATIONS

For a fair comparison of two different (fuel) cases, in terms of radiotoxicity or decay heat production, the cases should be equivalent in terms of reactor operating conditions. One way to make two subcases equivalent is to look at the k_{inf} of both cases. This k_{inf} is the ratio of the neutrons that are produced by fission against the total neutron loss due to absorption. (van Dam, van der Hagen, & Hoogenboom, 2005) To create a nearly equivalent case the k_{inf} value should be equal over the burn-up domain and the generated power should be equal.

The difference between the two cases is the starting fuel of the burn-up calculation. The two cases are stated in Table 4.1, this makes it easier to refer to them.

Table 4.1: *Statement of the two analysed cases*

	Case Thorium	Case Uranium
Fuel	Th-232/U-233	U-238/U-235

To continue, it is important to choose a realistic fuel cycle conditions for one of the two cases and to use the k_{inf} to find an equivalent condition for the second case. In this work a starting condition is chosen for the Uranium case. These conditions are based on the specifications of the Chinese 2 x 250 MW_{th} HTR-PM demonstration plant (Zhang, Wu, Wang, Xu, Sun, & Dong, 2009). Table 4.2 gives all the important settings for the Uranium case used in the simulations.

Table 4.2: *Fuel cycle parameters for case Uranium*

	Case Uranium	Units
Average Burn-up	90	GWd/t_{hm}
Fuel Temperature	1000	K
Enrichment '*p*'	9	%
Number of TRISO particles	10000	-
Radius fuel kernel (pebble)	0.025	cm
Radius fuel zone (pebble)	2.5	cm
Heavy metal loading	6.2177	g
ρ(density) of heavy metal	9.66	g/cm^3
Irradiation time steps	15	-
Number of irradiations per time step	15	-
Irradiation time per irradiation	5	day
Total irradiation time	1125	day

The derivation of ρ, the density, will be given in Appendix B. As mentioned before, the average k_{inf} of case Thorium has to be more or less the same as the one of case Uranium. One way to achieve this is to adjust the enrichment of the fuel. This is a proper way because the enrichment influences the amount of neutrons and the neutron balance which effects k_{inf}. This is also the method used here. The starting conditions for case Thorium are exactly the same except the used fuel, the density and, for this moment the most important parameter, the U-233 weight fraction, *p*. which has to be set at the right value. For this reason, the k_{inf} is compared for several values of *p*, as shown in Figure 4.1.

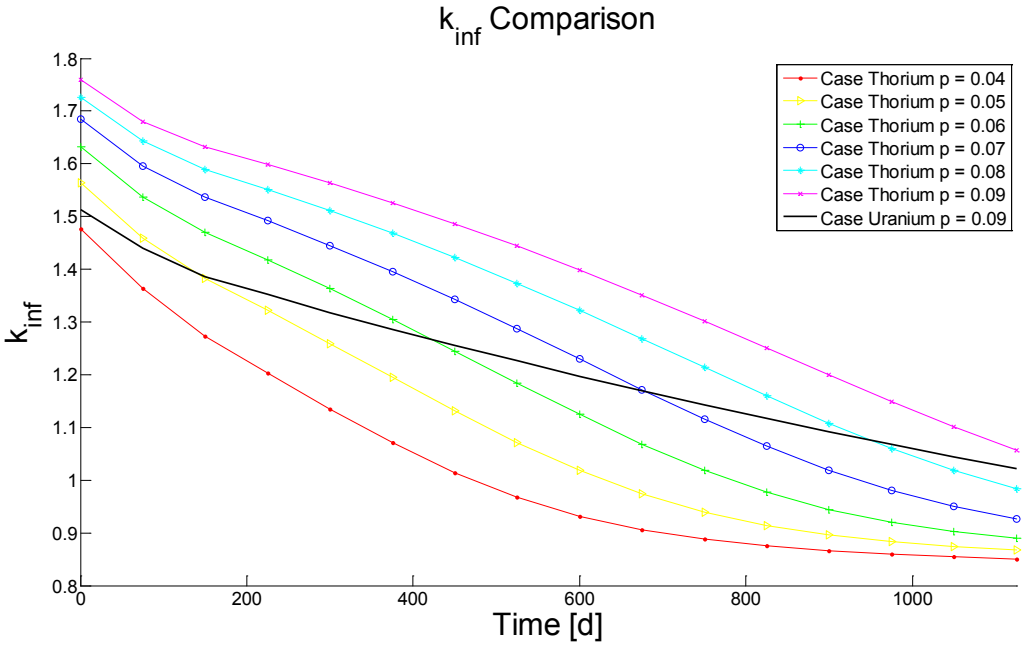

Figure 4.1: *k_{inf} comparison between Case Thorium and Case Uranium for different values of p, enrichment. The curves of case thorium are steeper than the (black) one of case uranium. This implies that it is impossible to find a case with exactly the same k_{inf}. However, this is possible when the average k_{inf} is taken into account.*

This graph shows the k_{inf} as a function of time with p values as a parameter. It is clear that it is impossible to find a value for p for case Thorium in such a way that the k_{inf} follows the same path as in case Uranium. Because the slope of case Thorium is always steeper than that of case Uranium. Therefore the comparison is changed to a comparison of the area under the graphs. The area beneath case Thorium, i.e. the average k_{inf}, has to be the same as that beneath case Uranium. The area under case Uranium lays in between the areas of case Thorium with p=0.06 and p=0.07. With use of interpolation the optimal p value for case Thorium to be equal to case Uranium is found as 0.06523. Figure 4.2 shows the k_{inf} comparison for case Thorium with this p value and case Uranium with the settings of Zhang et al (2009).

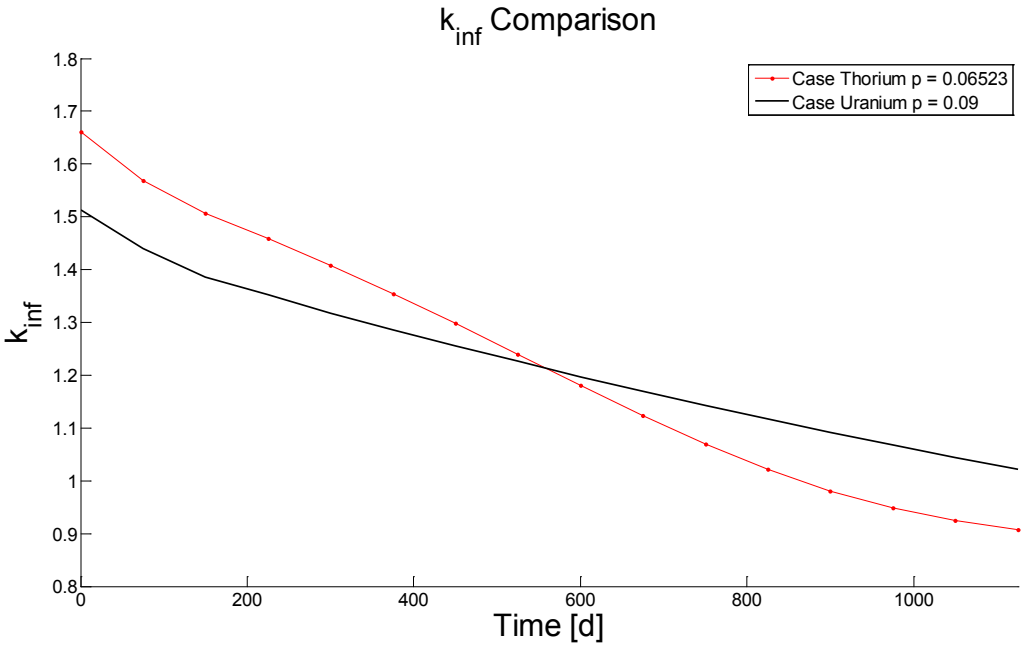

Figure 4.2: *Comparison at k_{inf} between case Thorium with the optimal p value and case Uranium with the settings of Zhang et al (2009). The area under the two graphs is equal.*

At this stage the configurations of case Thorium and case Uranium are set and the main comparisons can be made. First, a short overview of the main settings of case Thorium and case Uranium is given in Table 4.3.

Table 4.3: *Overview of the fuel cycle parameters of both case Thorium and Case Uranium*

	Case Thorium	Case Uranium	Units
Average Burn-up	90	90	GWd/t_{hm}
Fuel Temperature	1000	1000	K
Enrichment *'p'*	6.523	9	%
Number of TRISO particles	10000	10000	-
Radius fuel kernel (pebble)	0.025	0.025	cm
Radius fuel zone (pebble)	2.5	2.5	cm
Heavy metal loading	5.7858	6.3225	g
ρ(density) of heavy metal	8.84	9.66	g/cm^3
Irradiation time steps	15	15	-
Number of irradiations per time step	15	15	-
Irradiation time per irradiation	5	5	day
Total irradiation time	1125	1125	day

One of the important parameters in this table is the heavy metal density (ρ) inside the pebble. Appendix B is a derivation of this ρ for the different cases.

4.1.2 COMPARISONS

At this stage all the important parameters are defined and the results can be compared. The data used for the comparisons have been provided with use of the described program *decay_loop*. The main input parameters are set, as in Table 4.3, in order to simulate both case Thorium and case Uranium. Figure 4.3 and Figure 4.4 show the results with respect to the radiotoxicity and decay heat respectively. From these two figures general conclusions can be drawn about the comparison between case Thorium and case Uranium. Firstly, there is a significant difference, both in radiotoxicity and heat production, by the different isotopes. At the short term (100 years), the fission products dominate both the radiotoxicity and heat production for case Thorium, whereas for case Uranium the actinides have a significantly higher contribution. This difference will be discussed on the basis of Figure 4.5 and Figure 4.6, which shows the radiotoxicity and heat production as function of time. Secondly the great differences in absolute values for both radiotoxicity and heat production after 1000 year are remarkable and are also analysed further after Figure 4.5 and Figure 4.6.

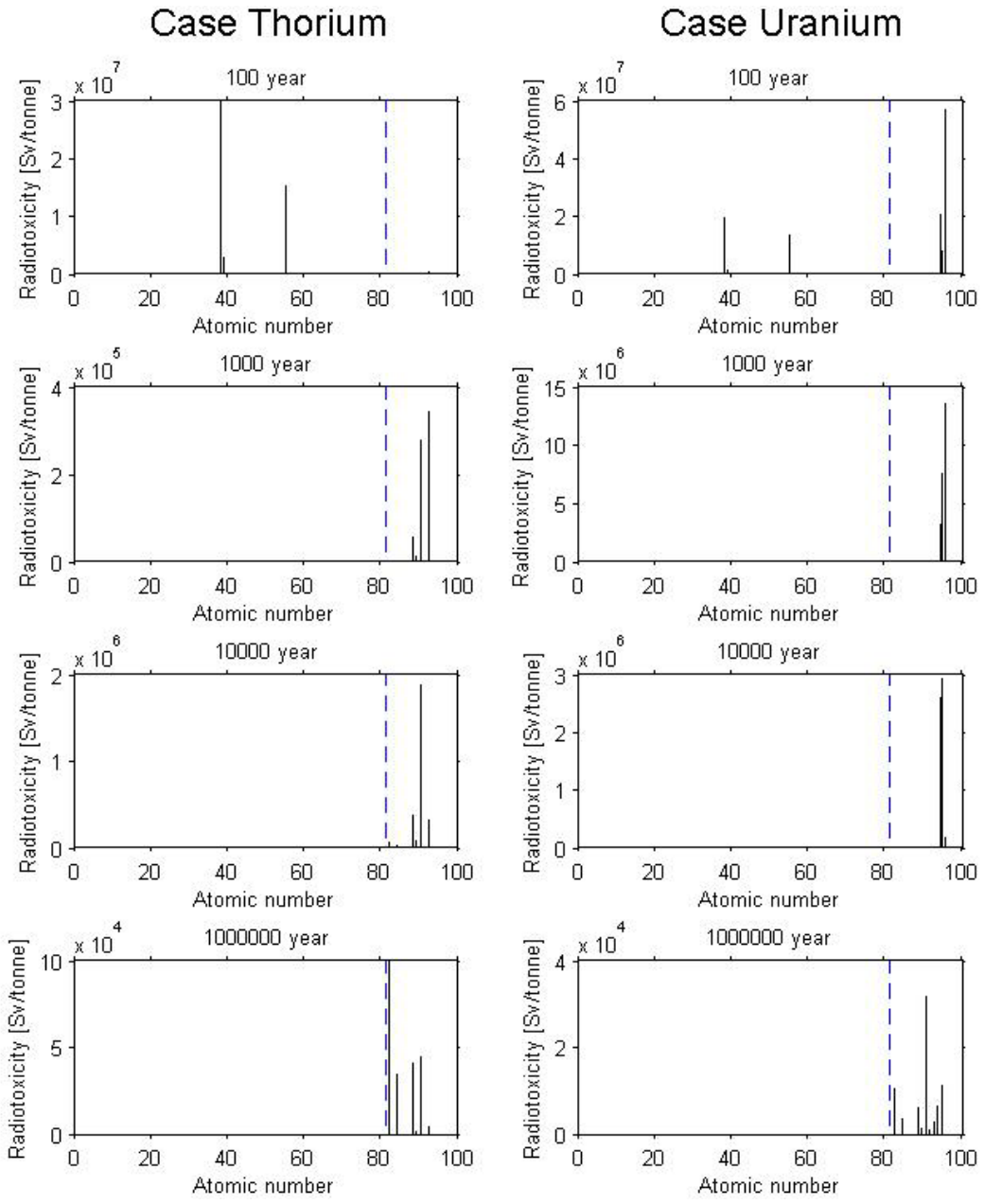

Figure 4.3: *Comparison of the radiotoxicity per tonne initial heavy metal loading of Case Thorium and Case Uranium for different storage times. The blue vertical dashed line divides the fission products (left) and actinides (right). Mind the different y-axes on the second row of plots.*

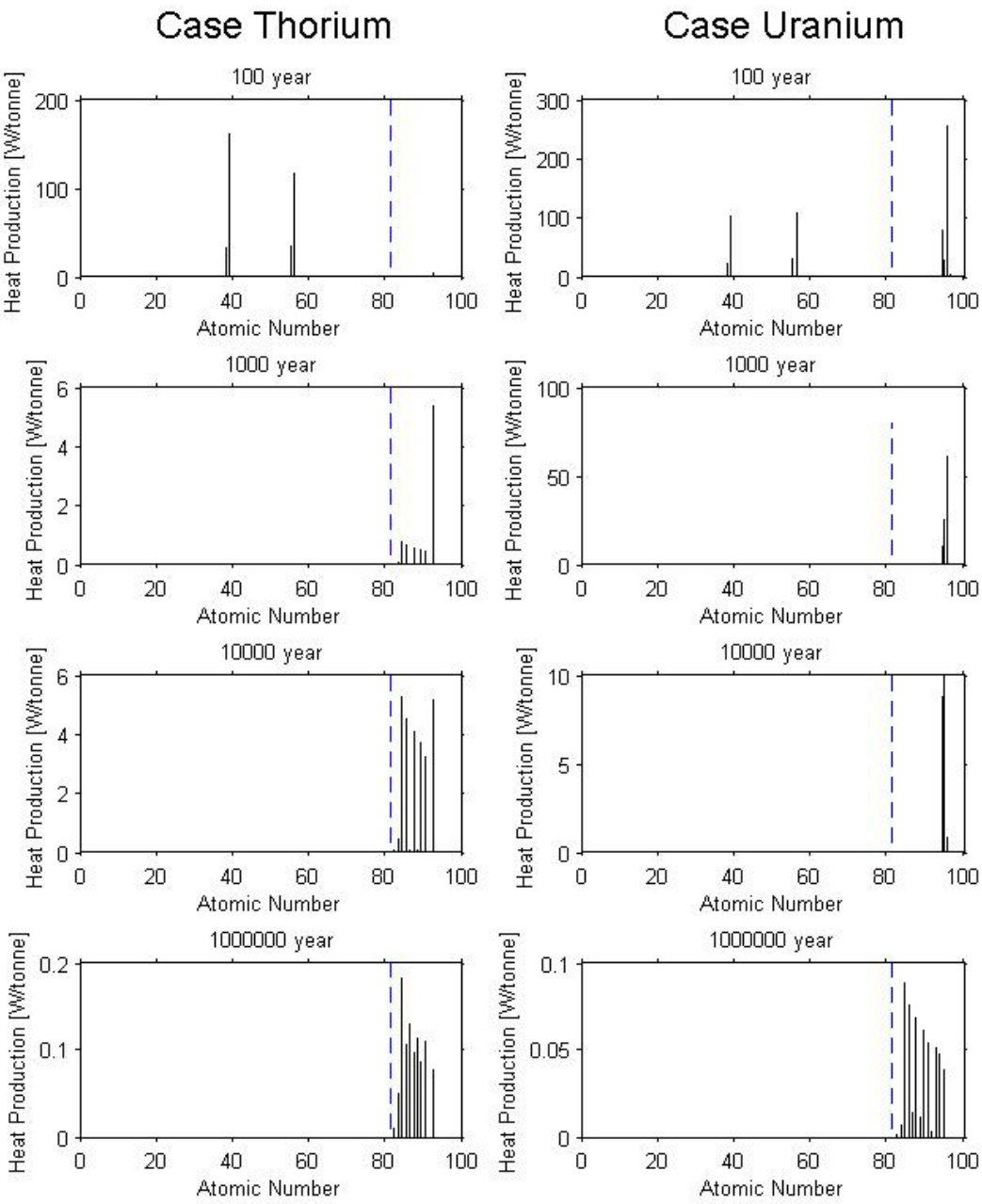

Figure 4.4: *Comparison with respect to heat production per tonne initial heavy metal loading of Case Thorium and Case Uranium for different storage times. The blue vertical dashed line divides the fission products (left) and actinides (right).*

To have a better insight on the radiotoxicity and heat production as a function of time, plots are made in Figure 4.5 and Figure 4.6, containing the total number of isotopes (blue), the fission products only (red) and the actinides only (black) in the first row of plots. The contribution of several fission products and actinides is the second and third row to visualize some interesting differences between the two cases. Fission products and actinides with contributions larger than a pre-set cut-off value are shown. This is based on an analysis of all the contributing isotopes and only the most contributing isotopes where plotted. This selection of isotopes turned out to be equal to the selection made by Ashley et al (2014)

First, the time of which the contribution of the actinides exceeds the contribution of the fission products is different. For case Thorium this happens after around 300 years in contrast to case Uranium, where this point is at around 70 years. Though this is remarkable, it is not that important for this study, because the interesting time scale for long term storage is way higher than these hundreds of years.

The second remarkable difference is more important with respect to the storage of the nuclear waste, i.e. the radiotoxicity and heat production increase again between a storage time of 1000 years and 100,000 years in case Thorium. The increase is only due to the actinides, the fission products are no longer significant at this timescale. After the increase, case Thorium has practically the same value as case Uranium. When having a closer look to the actinides, it becomes clear that the increase is roughly caused by the Th-229 produced from the U-233 by decay. The same increase of radiotoxicity and produced heat due to Th-229 seems to happen in case Uranium, but the concentration of Th-229 is very low, so this has scarcely any effect on the total radiotoxicity and decay heat production. At this time the other actinides contribute no longer, whereas they did in case Thorium at the moment of the maximum.

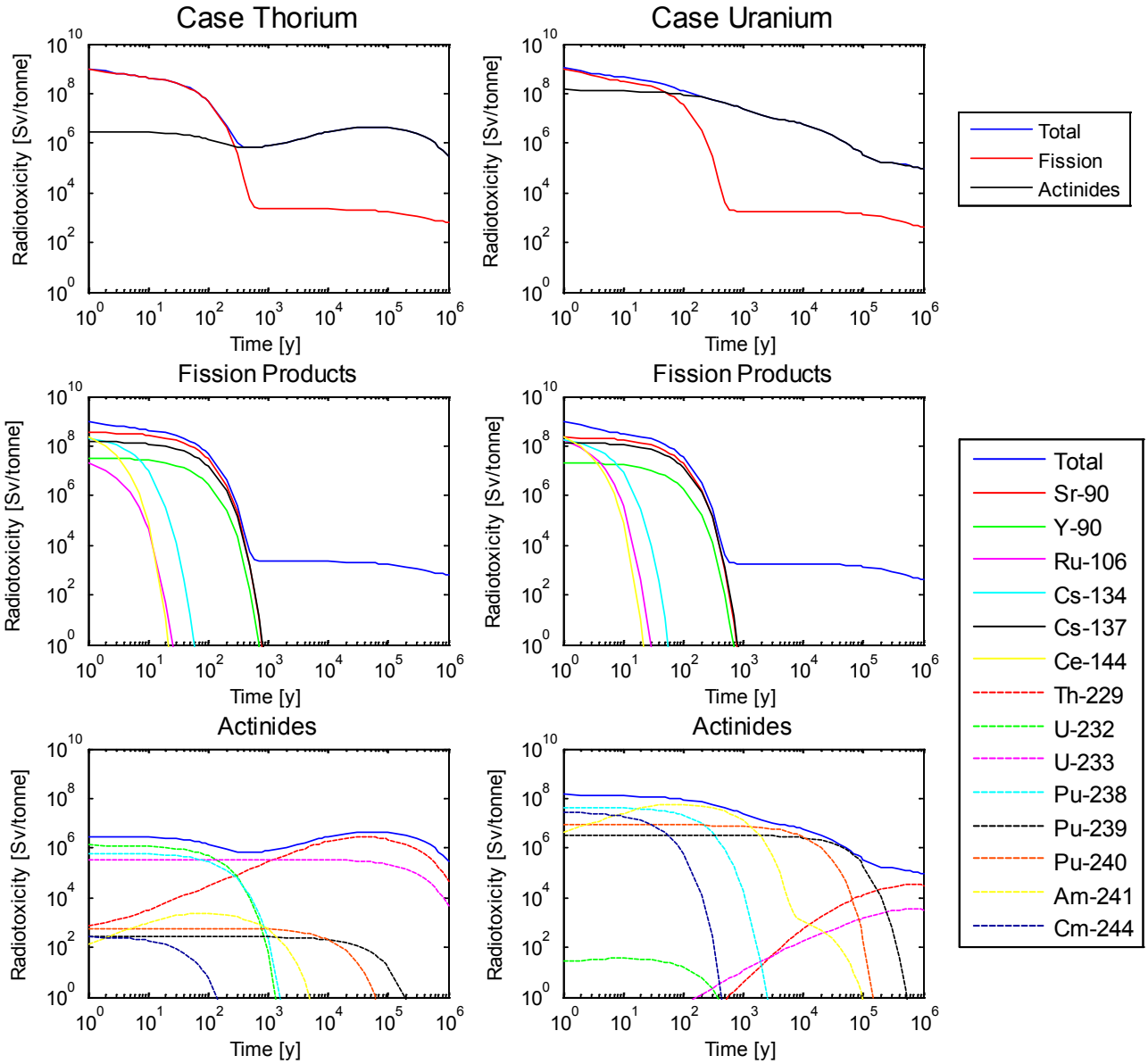

Figure 4.5: *Radiotoxicity per tonne heavy metal loading as a function of time. The first row shows the sum of the contribution of all isotopes (blue), the sum of the contribution of the fission products (red) and the sum of the contribution of the actinides (black). The second row shows the contribution of several interesting fission products and the total contribution of the fission products (blue). The last row shows the contribution of the most contributing actinides and the total contribution of the actinides (blue).*

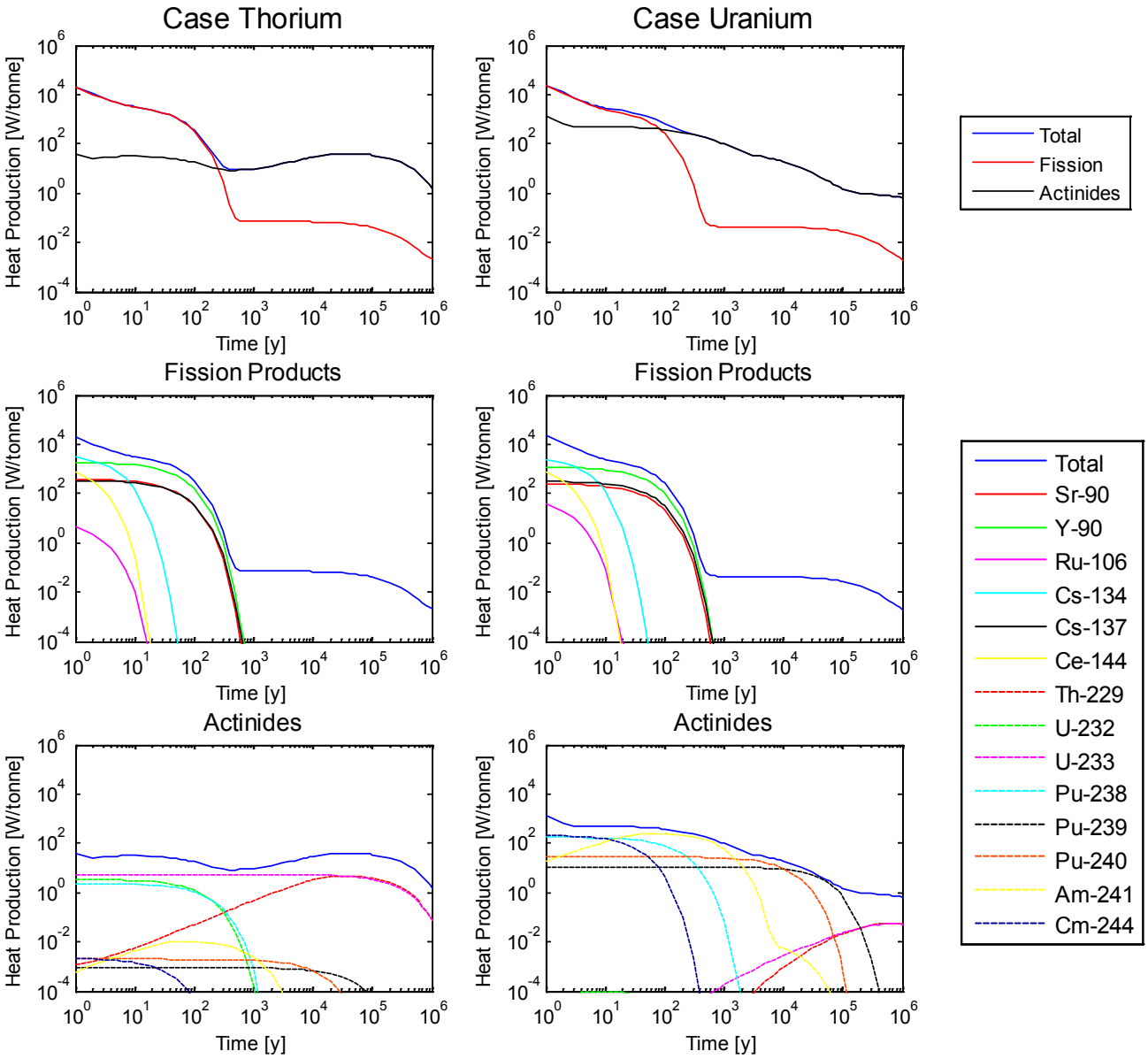

Figure 4.6: : *Heat production per tonne heavy metal loading as a function of time. The first row shows the sum of the contribution of all isotopes (blue), the sum of the contribution of the fission products (red) and the sum of the contribution of the actinides (black). The second row shows the contribution of several interesting fission products and the total contribution of the fission products (blue). The last row shows the contribution of the most contributing actinides and the total contribution of the actinides (blue).*

The first 100 years after removing the depleted nuclear fuel from the core, the waste is typically stored in a short term waste storage place, as mentioned in the introduction (NEA, 2007). On this short time scale the greatest difference between case Thorium and case Uranium is the absolute value of the contribution of the actinides to the radiotoxicity and the decay heat. The radiotoxicity due to the actinides seems to be a bit lower in case Thorium. As mentioned, later on these levels become almost the same, due to the increase after 1000 years of storage. The difference on short term, 100 years, in absolute values is quite interesting. The mean value of the heat production due to the actinides in case Thorium is 27 [W] and for case Uranium it is 514 [W]. A difference of 487 [W] heat produced per tonne heavy metal. While after 1 million years the difference is only 10 [W]. However, the average heat production over the first 100 years due to the fission products is in both cases almost 4000 [W], this means that the advantage in heat production in case Thorium caused by the actinides would only have a significant effect if the actinides and fission products are chemically separated before storage, but that doesn't solve the problem of heat production during storage. In order to obtain progress in the decay heat production, actinide recycling is needed.

The final conclusion that can be drawn from Figure 4.5 and Figure 4.6 has to do with the moment of switching from short term to long term storage. The maximum value of the 'hill' between 100 and 100,000 years can act as an interesting benchmark on the moment of switching from short term to long term storage. It was mentioned in the introduction chapter that this moment was normally at 100 years. Looking at figure 4.6 it can be concluded why this moment is actually chosen. The amount of heat produced at this moment is slightly higher than the maximum, between 1000 and 100,000 years. The strategy is to choose a switching moment that is almost equal to this maximum value, so that no further improvements have to be done on the long term storage in order to prevent for decay heat production. The counterpart of this strategy is that the radiotoxicity will be a bit higher at this moment, so additional radiation protection is needed.

4.2 SINGLE PEBBLE – ACTINIDE RECYCLING SIMULATIONS

The two most realistic options of the three types of actinide recycling mentioned in the theory chapter will be discussed in this paragraph, starting with the theoretical ($k_{inf} < 1$) thorium breeder configuration. Thereafter the more realistic ($k_{inf} > 1$) plutonium closed uranium cycle configuration will be analysed, which is an extension of the thorium breeder configuration. The idea is to compare the radiotoxicity and the decay heat production of both configurations with the single pebble simulations without recycling of case Thorium as well as with each other, to see if they can reduce the radiotoxicity per unit energy produced. Before the preparation of the parameters and the actual comparisons a verification on the reason for recycling is done. It will also show why the recycling of the specific isotope U-233 is chosen.

4.2.1 ACTINIDE RECYCLING VERIFICATION – *'BIFTOX'*

The graphs of paragraph 4.1 show that the radiotoxicity and decay heat production are dominated by the fission products on the short term and by the actinides on the long term. The long term storage (> 100 years) is the interesting time scale for recycling because here the long lived actinides play a greater role than the short lived fission products. The graphs of paragraph 4.1, without recycling, just showed the contribution of each single isotope. However, it is interesting to see the origin of all these long lived actinides, a plot of the mothers including all their daughters. The daughters were namely formed out of their mothers due to different decays. This is interesting in the case of recycling, because if the most contributing mother isotopes are recycled, also the 'daughter effects', e.g. Th-229, are reduced.

To make a graph which contains the contributions of the daughter products for each mother nuclide use is made of a table of the mother nuclides and their daughters for the most important actinides. The tables are generated with a program called BIFTOX which has been written by J.L. Kloosterman and makes use of the dose coefficients of nuclides of Appendix C (Kloosterman, 1996). The used values are given in Table D.1 of Appendix D. A simple script is used to convert first the units of the values of table E.1 from *Sv/mole* to *Sv/g* by dividing them by the associated molar masses. This is followed by a multiplication with the concentrations generated with the burn-up code.

The left part of Figure 4.7 is added in order to verify the BIFTOX results with the simulated ORIGEN-S results. It is clear that the two methods produces nearly the same graphs, the small deviations are due to the rougher time interval in the BIFTOX tables than in ORIGEN-S. The right part of Figure 4.7 shows the most radiotoxicity producing nuclides, mothers and daughters together, by a configuration of case Thorium without actinide recycling stated in paragraph 4.1. The BIFTOX results show that U-233 is indeed an important actinide in the production of radiotoxicity. So the choice of recycling the U-233 is very beneficial with respect to the radiotoxicity of the nuclear waste.

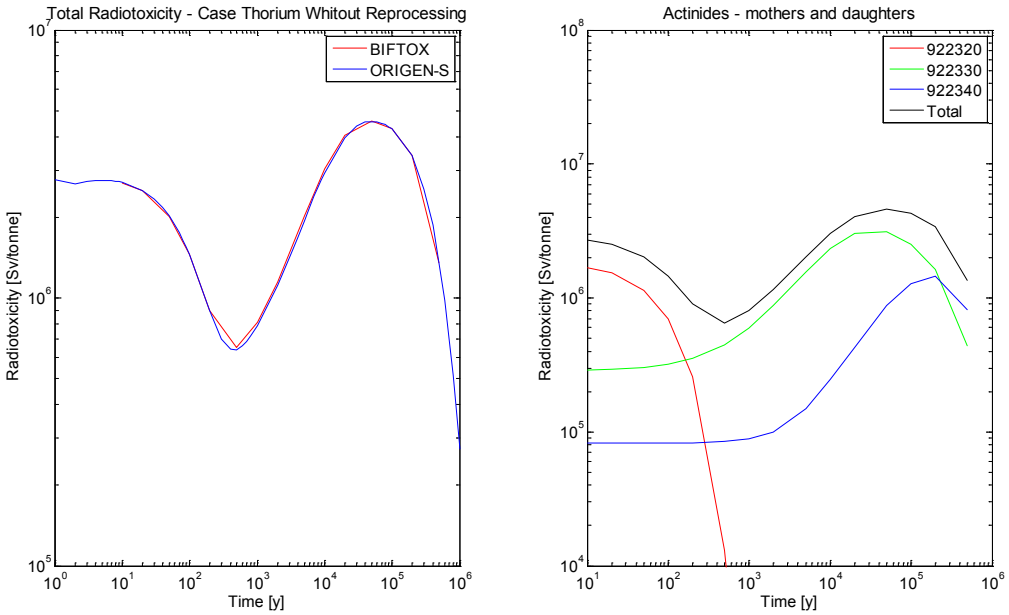

Figure 4.7: *[Left] Validation of the BIFTOX program by comparing it with the graph generated by the simulation of ORIGEN-S, see paragraph 4.1, both graphs are generated with use of the data produced for the thorium non-critical breeder pebble configuration without actinide recycling. [Right] BIFTOX plot for the actinides in the thorium non-critical breeder configuration without actinide recycling.*

4.2.2 PARAMETER PREPARATIONS – THORIUM NON-CRITIAL BREEDER CONFIGURATION

In order to get a closed fuel cycle at least the amount of U-233 that was added in the initial pebble has to be produced every burn-up cycle. Although $k_{inf} < 1$ a thorium breeder configuration is used. After one single burn-up cycle (case Thorium simulated in paragraph 4.1) 1.62 % of U-233 per tonne initial heavy metal is left, while 6.523 % was added to the initial pebble. This means that more U-233 has to be added, which was not the idea of this configuration so a lower enrichment, weight fraction, of U-233 is required, in order to satisfy the conditions of breeding. A range of enrichment values was tested in order to find the starting configuration that comes closest to a closed U-233 cycle. This was not the only adjustment made, also the pebble loading was changed to 30 gram, which is the maximum heavy metal loading for a fuel pebble, in order to increase the chance of neutron capture by the thorium, which leads to U-233 production. (Wols, Kloosterman, & Lathouwers, 2012) At the end 2.39 % enrichment turned out to be the p-value for which the produced U-233 was more or less the same as the initial loading. However, it was already mentioned in the theory chapter that it was not possible to get this configuration critical. Figure 4.8 shows the graphic evidence for this. It shows that the k_{inf} of the thorium breeder pebble case is only above one in the first few days, so a reactor design cannot be critical. Despite of the non-criticality of the system a comparison between this recycling option and the case without recycling will be made in order to see if it could have been useful to reprocess in this way.

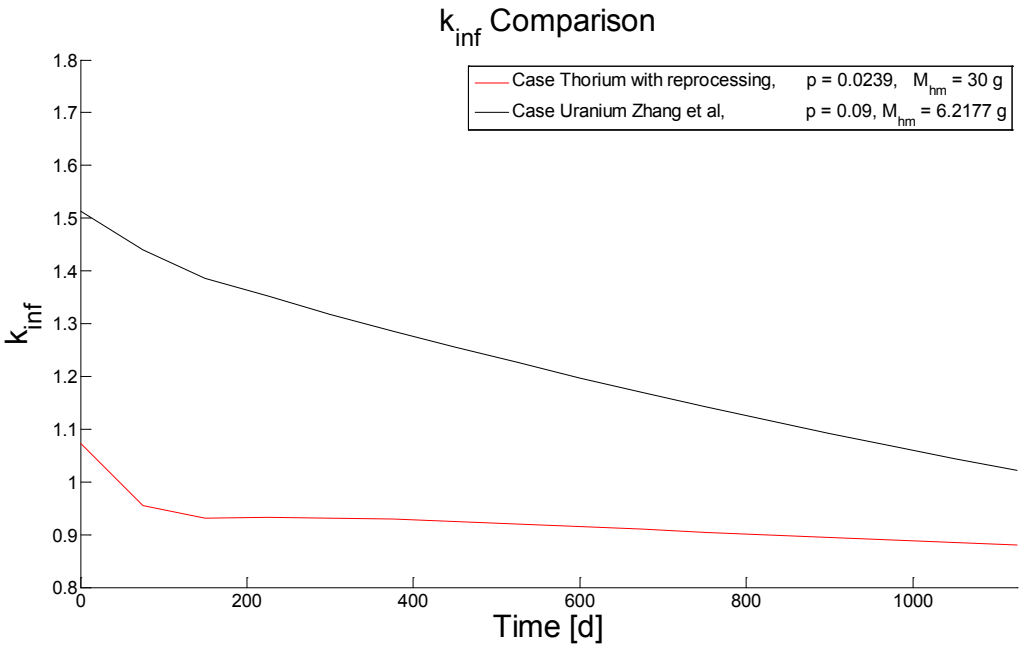

Figure 4.8: *k_{inf} comparison between the thorium non critical breeder configuration with the optimal p value and case Uranium with the settings of Zhang et al (2009). Equality of the cases is not reached.*

At this stage the starting conditions for the actinide recycling on the thorium non-critical breeder configuration can be stated. They can be found in Table 4.4. After each burn-up the next recycling step will start with these initial conditions. The only difference between a certain recycling step and the first step is the (partial) recycling of the Th-232, U-233 and the minor actinides above.

Table 4.4: *Fuel cycle parameters thorium non-critical breeder recycling configuration*

	Case Actinide recycling Th	Units
Average Burn-up	90	GWd/t_{hm}
Fuel Temperature	1000	K
Enrichment *'p'*	2.39	%
Number of TRISO particles	51910	-
Radius fuel kernel (pebble)	0.025	cm
Radius fuel zone (pebble)	2.5	cm
Heavy metal loading	30	g
ρ(density) of heavy metal	8.83	g/cm^3
Irradiation time steps	15	-
Number of irradiations per time step	15	-
Irradiation time per irradiation	5	day
Total irradiation time	1125	day

4.2.3 PARAMETER PREPARATIONS – PLUTONIUM CLOSED URANIUM CYCLE ADDITION

The second recycling option was the plutonium closed uranium cycle as in the thorium non-critical breeder configuration, where the heavy metal loading is decreased and a certain amount of reactor grade plutonium is added to reach criticality as well as a closed U-233 system. It was quite hard and almost impossible to find a starting configuration of the reactor grade plutonium, the U-233 and the Th-232 in such a way that the k_{inf} would on average be the same as the k_{inf} in the case of the HTR-PM of Zhang et al (2009). This did not succeed because the average k_{inf} remained below the HTR-PM case. Therefore a different approach was taken. Use was made of some calculations on the HTR-PM al done by Gert-Jan Auwerda for k_{eff}/k_{inf}, which is equal to the probability of leakage of the neutrons. A value of 0.89 was found for k_{eff}/k_{inf}, this would mean that the k_{inf} has to be at least 1.11 in order to compensate the leakage of 11 percent.

The starting condition criteria are a closed uranium loop and an averaged k_{inf} of at least 1.11 percent. Still this was quite hard to find and unachievable in the time of this project. For this reason a starting condition yielding a closed uranium loop with an average k_{inf} of 1.09 was chosen. See Figure 4.9. Leakage in a HTR-PM output can still be reduced by using larger core dimensions.

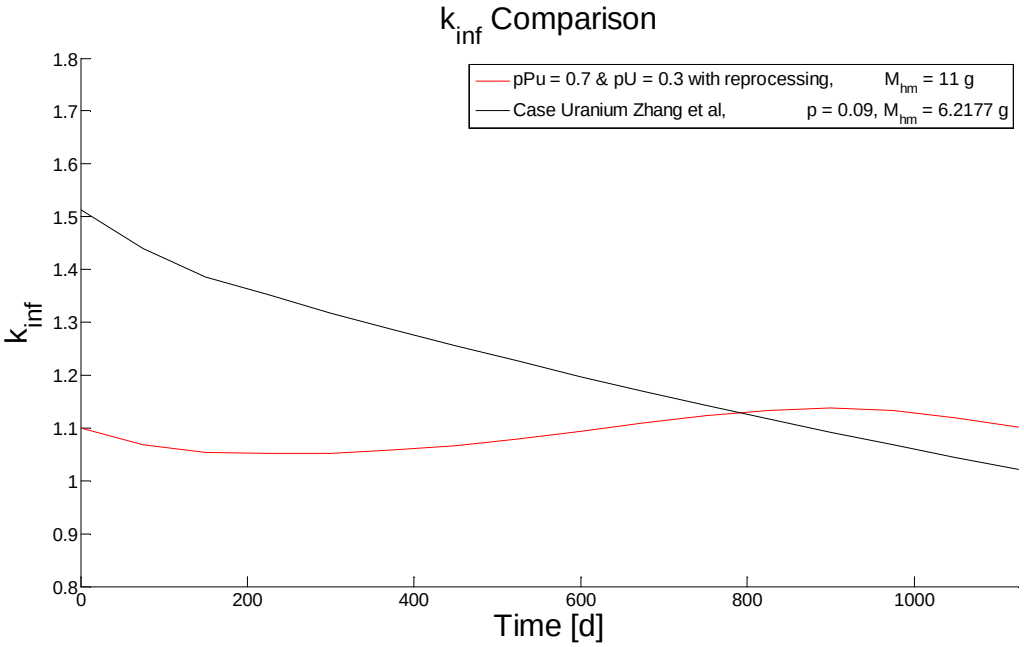

Figure 4.9: *k_{inf} comparison between the plutonium closed uranium recycling configuration and case Uranium with the settings of Zhang et al (2009). Equality of the cases is nearly reached.*

Now, the starting conditions of the actinide recycling based on the Plutonium closed uranium cycle configuration can be defined. They can be found in Table 4.5. After each burn-up the next recycling step will start with these initial conditions. The only difference between a certain recycling step and the first step is the (partial) recycling of the Th-232, reactor grade Plutonium (Pu-238, Pu-239, Pu-240, Pu-241 and Pu-242), U-233 and the minor actinides above.

Table 4.5: *Starting condition plutonium closed uranium cycle addition configuration*

	Case Actinide Recycling Pu-RG	**Units**
Average Burn-up	90	GWd/t_{hm}
Fuel Temperature	1000	K
Enrichment		
- *'pPu'*	7	%
- *'pU'*	3	%
Number of TRISO particles	17525	-
Radius fuel kernel (pebble)	0.025	cm
Radius fuel zone (pebble)	2.5	cm
Heavy metal loading	11	g
ρ(density) of heavy metal	8.83	g/cm^3
Irradiation time steps	15	-
Number of irradiations per time step	15	-
Irradiation time per irradiation	5	day
Total irradiation time	1125	day

4.2.4 COMPARISONS

To make realistic and fair comparisons between the different recycled simulations, the radiotoxicity and decay heat production are evaluated per unit energy as in paragraph 4.1. A unit energy is defined as the amount of energy produced out of one tonne initial heavy metal after one burn-up cycle, namely 90 *GWd/t*.

In order to avoid confusion for the reader, the decay time will be the same for both the non-reprocessed and reprocessed cases. So, an assumption was made that the nuclear waste would not decay in the first few years, the time the actinide recycling takes. This assumption is allowed, because the main focus here is on the long lived actinides, which hardly decay during 100 years. The main results obtained with recycling are given in Figure 4.10.

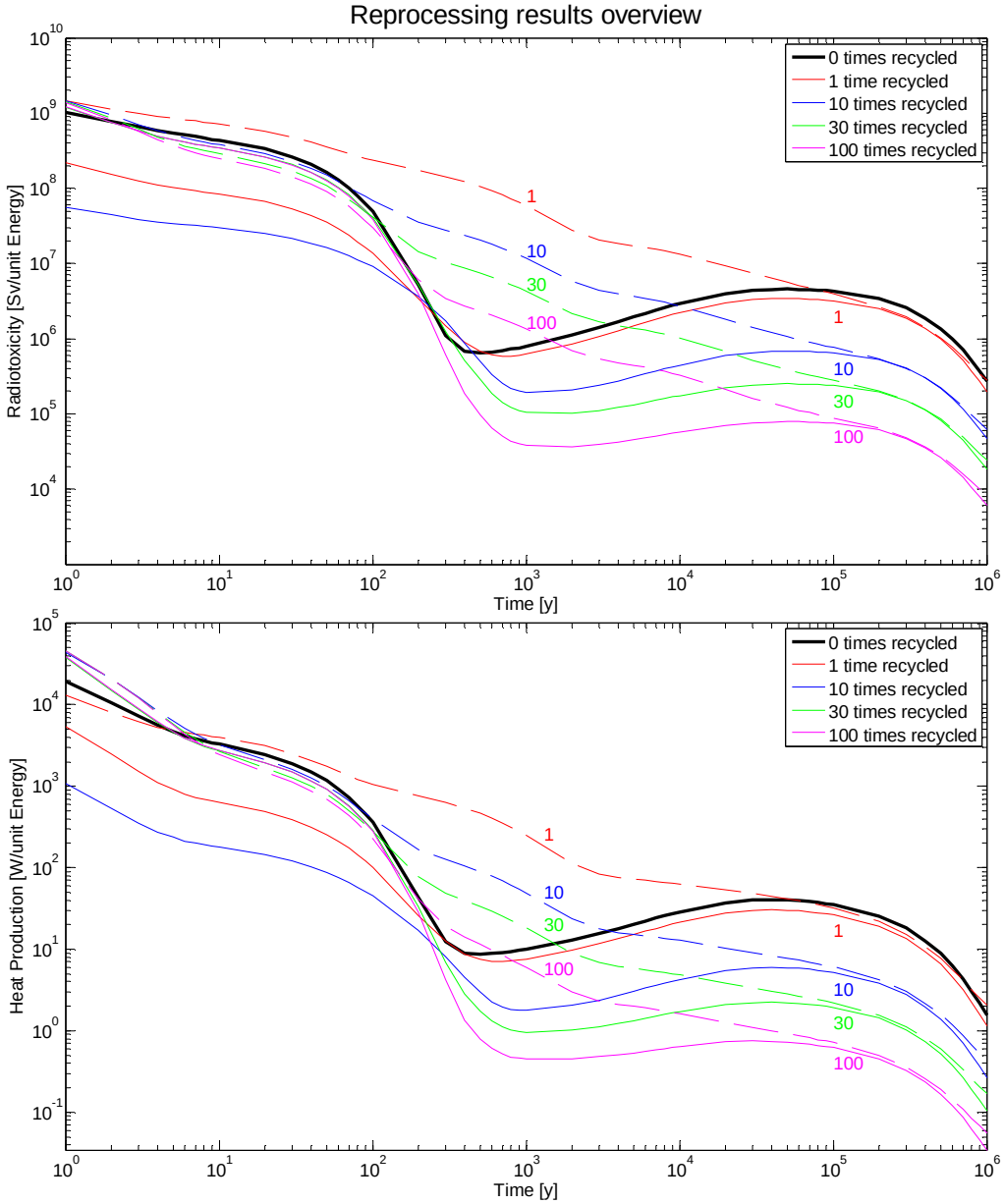

Figure 4.10: *[Top] Radiotoxicity per unit energy (90 GWd) produced over time. [Bottom] Heat Production per unit energy over time. The solid black line represents Case Thorium that is equivalent to Zhang et al (2009), as obtained in the first part of the results without actinide recycling. The solid coloured lines represent the thorium non-critical breeder configuration and the dashed coloured lines represent the plutonium closed uranium cycle configuration.*

Figure 4.10 shows that actinide recycling can have a great impact on the radiotoxicity and heat production. Comparing the two different recycling techniques it becomes clear that the thorium non-critical breeder configuration (solid line) would give a better result than the plutonium closed uranium cycle (dashed line) does. However, this option is not realistic as mentioned earlier. When having a closer look on the more realistic plutonium closed uranium cycle it is striking that 100 times recycling would give a decrease of factor 100 in radiotoxicity after 1 million year, while it equals the level of radiotoxicity of the non-reprocessed thorium case after about 100 years, which is exactly the time scale on which the nuclear waste will move from the short term to the long term storage. So this seems to be a quite good result.

A final look at Figure 4.10 results in a the same possible optimal time of switching from short to long term storage as in the case without actinide recycling. Looking at the case of one time recycling, it becomes clear that the 'hill' in the graph of decay heat production will have its maximum at about 40 [*W*]. The waste will not pass this value during long term storage, so it seems to be a reasonable option to switch from short to long term at the moment this value of 40 [*W*] is reached first, at a decay time of around 200 years. The moment of switching will shift from 100 years to somewhere between 200 and 600 years, depending on the number of recycling steps. Choosing this switching point strategy ensures that no extra improvements for heat production have to be made, when choosing the switch at the moment of minimum heat production and radiotoxicity. The counterpart of this strategy again is the higher value of radiotoxicity at this moment, so additional radiation protection is needed.

The final result of this thesis is demonstrated in Table 4.6 and Table 4.7. The differences Δ in concentration after the final actinide recycling cycle and radiotoxicity and decay heat production after 1 million years of decay owing to an increase in amount of recycling steps are given. Only the actinides are taken into account.

Table 4.6: *Differences (Δ) in concentration after the final actinide recycling cycle and radiotoxicity and decay heat production after 1 million years of decay owing to an increase in amount of recycling steps while using the plutonium closed uranium configuration. All values for concentration, radiotoxicity and decay heat are per single step, e.g. the radiotoxicity for the case of 30 recycling steps is divided by 31 (the total number of burn-ups).*

# recycling steps	Concentration *[atoms/barn*cm]*	Δ	Radiotoxicity *[Sv/tonne]*	Δ	Decay Heat *[W/tonne]*	Δ
0	$2.0428 \cdot 10^{6}$	-	$1.0272 \cdot 10^{4}$	-	0.1511	-
1	$1.0641 \cdot 10^{6}$	$9.7870 \cdot 10^{5}$	$4.2615 \cdot 10^{4}$	$-3.2343 \cdot 10^{4}$	0.3820	−0.2309
10	$0.1958 \cdot 10^{6}$	$8.6827 \cdot 10^{5}$	$0.8729 \cdot 10^{4}$	$3.3886 \cdot 10^{4}$	0.0786	0.3034
30	$0.0700 \cdot 10^{6}$	$1.2579 \cdot 10^{5}$	$0.3550 \cdot 10^{4}$	$5.1787 \cdot 10^{3}$	0.0306	0.0479
100	$0.0216 \cdot 10^{6}$	$4.8468 \cdot 10^{4}$	$0.1260 \cdot 10^{4}$	$2.2899 \cdot 10^{3}$	0.0102	0.0205

Table 4.7: *Differences (Δ) in concentration after the final actinide recycling cycle and radiotoxicity and decay heat production after 1 million years of decay owing to an increase in amount of recycling steps while using the thorium non-critical breeder configuration. All values for concentration, radiotoxicity and decay heat are per single step, e.g. the radiotoxicity for the case of 30 recycling steps is divided by 31 (the total number of burn-ups).*

# recycling steps	Concentration *[atoms/barn*cm]*	Δ	Radiotoxicity *[Sv/tonne]*	Δ	Decay Heat *[W/tonne]*	Δ
0	$2.0428 \cdot 10^{6}$	-	$1.0272 \cdot 10^{4}$	-	0.1511	-
1	$1.0697 \cdot 10^{6}$	$0.9731 \cdot 10^{5}$	$0.7726 \cdot 10^{4}$	$2.5461 \cdot 10^{3}$	0.1137	0.0374
10	$0.1966 \cdot 10^{6}$	$8.7312 \cdot 10^{5}$	$0.1968 \cdot 10^{4}$	$5.7583 \cdot 10^{3}$	0.0276	0.0861
30	$0.0700 \cdot 10^{6}$	$1.2661 \cdot 10^{5}$	$0.0795 \cdot 10^{4}$	$1.1732 \cdot 10^{3}$	0.0107	0.0169
100	$0.0215 \cdot 10^{6}$	$4.8512 \cdot 10^{4}$	$0.0252 \cdot 10^{4}$	$5.4343 \cdot 10^{2}$	0.0033	0.0074

It is interesting to see that in both actinide recycling configurations the Δ tends to decrease but still stay positive when the number of recycling steps increases. This is the desired result, because it shows the reduction in radiotoxicity and decay heat production due to recycling.
However, there are some outliers, which can be explained. Namely the negative values for Δ when the waste is reprocessed once; this is due to the addition of the radiotoxic reactor grade plutonium, after a few recycling steps this effect disappears i.e. after 10 recycling steps.

Chapter 5

CONCLUSIONS AND RECOMMENDATIONS

The main questions of this survey were firstly: Does a thorium fuelled pebble bed reactor lead to a lower radiotoxicity and heat production of the waste than an uranium fuelled one? And secondly: How are the radiotoxicity and heat production at the waste affected by recycling of the most radiotoxic minor actinides? The k_{inf} was used as a comparing tool in order to have equal cases, an equal k_{inf} over the burn-up domain means that the neutron balances are equal. All cases were chosen in such a way that they were comparable to the specifications of the HTR-PM of Zhang et al (2009). Two types of recycling where compared in this work; the thorium non-critical breeder configuration and the plutonium closed uranium cycle configuration. The first one recycled all the U-233 and used the breeding ability of thorium, unless the fact that it couldn't become critical. The second recycling option replaced some of the thorium by reactor grade plutonium, in order to reach criticality.

5.1 THORIUM COMPARED TO URANIUM WITHOUT ACTINIDE RECYCLING

The first part of the investigation was focused on the comparison of the radiotoxicity and decay heat between thorium and uranium, both without actinide recycling. At the long term storage there is not a big difference noticeable between case Thorium and case Uranium. The results show a lower radiotoxicity when looking at the actinides of case Thorium, as expected, due to the lower chance on production of highly radiotoxic minor actinides since Th-232 has a lower mass number than U-238. The same conclusions can be drawn from the heat production. The uranium fuel cycle produces slightly less heat per ton heavy metal after 1 million years. However, on the short term, after 100 years, the thorium fuel cycle seems to be more favourable. Since this is the timescale on which short term storage is converted into long term storage, this seems to be a very interesting property of the thorium fuel cycle. The same drop after 100 years takes place in the radiotoxicity. So, the main conclusion of this first part of the survey is that the thorium fuel cycle leads to an overall decrease in radiotoxicity in the long term and an interesting drop in radiotoxicity and heat production after 100 years, the timescale of waste transfer from short to long term storage. This makes it easier and less expensive to deal with, because less (advanced) shielding is needed. However, there is a noticeable increase of radiotoxicity and decay heat production after the first 100 years. This should be taken into account in the construction of the long term storage. Which can be done by choosing the moment of switching from short term to long term at the moment the heat production reaches the first time the maximum level during long term storage. By choosing this strategy no extra improvements has to be made on the long term storage. This leads to a shift in short term storage from 100 years to somewhere between 200 and 600 years, depending on the number of recycling steps.

5.2 ACTINIDE RECYCLING

The actinide recycling simulations performed in the second part were only focused on the thorium fuel cycle, since this seems to be the most promising fuel cycle as mention in the previous paragraph. It can be concluded that the increase in radiotoxicity and decay heat production between 100 and 100,000 years was reduced in both recycling methods investigated. In the thorium non-critical breeder configuration this increase totally disappears whereas in the uranium case it is reduced a bit. So, the first conclusion is that actinide recycling can reduce the radiotoxicity and decay heat production after in the long term storage Furthermore, the amount of produced decay heat per unit energy is the same or lower than that produced in the case without actinide recycling in the long term storage. The advantage discussed in the previous paragraph still applies, switching from short to long term storage at the first moment the heat production reaches the maximum value of the long term storage is still a good idea. So, it can be concluded that the recycling does not have a worse effect at the time of switching from short term to long term storage and that the total radiotoxicity and decay heat production per unit energy decreases.

5.3 RECOMMENDATIONS

During this work some assumptions and simplifications have been made in order to simplify the actinide recycling model in order to fit within the limited scope of the present analysis. Therefore, results can be improved by better assumptions or more complex models to the script. The following list will give an overview of some possible future work on this topic.

- Firstly, decay has to be added to the stored fission products that are now just saved every recycling step and added to the concentration vector after the last recycling step. Especially for cases with many recycling steps this can lead to an unrealistic result. When decay of the temporary stored fission products is taken into account after each recycling step, the resulting concentration vector after the final recycling step will be more realistic. Also the radiotoxicity and decay heat production due to this temporal storage can be taken into account to say something meaningful about the needed specifications on storage facilities for this.
- Another simplification in this work is related to the cracking of the pebbles. As mentioned earlier this costs a few tenths of percent of the produced energy. When this energy cost is added to the model, the radiotoxicity per unit energy will be more realistic and precise. The question is whether it is still favourable to reprocess or not. Also a comparison can be made with other pebble cracking methods.
- To make the model more realistic, full core models instead of the single pebble model can be implemented. This would give other cross sections and also the k_{inf} will be different. Maybe this could lead to a full critical breeder design and also the required k_{inf} of at least 1.11 in the reactor grade closed uranium configuration.
- Lastly, the actinide recycling of the uranium fuel cycle has not been taken into account, it is possible that this would also lead to a reduction in radiotoxicity and decay heat production. By adding this to the model it is possible to make a total comparison between the thorium and uranium case, including several recycling steps.

BIBLIOGRAPHY

Ali, A., El-Nadi, Y., Daoud, J., & Aly, H. (2007). Recovery of Thorium (IV) from Leached Monazite Solutions using Counter-Current Extraction. *Int. J. Miner Process 81*, 217-223.

American Elements. (2014). *Thorium Oxide*. Retrieved May 28, 2014, from http://www.americanelements.com/thox.html

Ashley, S., & all, e. (2014). Fuel cycle modelling of open cycle thorium-fuelled nuclear energy. *Annals of nuclear energy 69*, 314-330.

Bos, A., Draaisma, F., & Okx, W. (2007). *Inleiding tot de Stralingshygiëne.* Den Haag: Sdu Uitgevers.

Dresselhaus, M., & Thomas, I. (2001). Alternative Energy Technologies. *Nature 414*, 332-337.

Eschbach, E., & Deonigi, D. (1966). *Possible Optimum Use of Thorium and Uranium Employing Crossed-progeny Fuel Cycles.* Richland Washington: Pacific Northwest Laboratory.

ESV Euridice EIG. (2010). *Boomse Klei.* Mol, Belgium: ESV Euridice.

Fütterer, M., von der Weid, F., & Klichmann, P. (2010). A High Voltage Head-End Process for Waste Minimization and Reproccessing of Coated Particle Fuel for High Temperature Reactors. *Proceedings of ICAPP*, 1825-1830.

Garvey, T. (2012). *Closing Yucca Mountain: Litigation Associated with Attempts to Abandon the Planned Nuclear Waste Repository.* Congressional Research Service.

Gauld, I., Hermann, O., & Westfall, R. (2009). *ORIGEN-S: Scale System Module to Calculate Fuel Depletion, Actinide Transumutation, Fission Product Buildup and Decay, and Associated Radiation Source Terms.* Oak Ridge, Tenessee: OAK Ridge National Laboratory.

Haynes, W. (2014-2015). *Handbook of Chemistry and Physics*. Retrieved August 20, 2014, from http://www.hbcpnetbase.com/: http://www.hbcpnetbase.com/

Hopkins, J., & Diven, B. (1962). Neutron Capture to Fission Ratios in U233, U235 and Pu 239. *Nuclear Science and Engineering 12*, 169-177.

IAEA. (2005). *Thorium Fuel Cycle - Potential Benefits and Challenges.* Vienna, Austria: IAEA 1450.

ICRP. (1990). *Annual Limits on Intake of RadioNuclides by Workers Based on the 1990 Recommendations.* Technical Report Publication 61, ICRP.

ICRP. (1994). *Dose Coefficients for Intakes of Radionuclides by Worker; Replacement of ICRP Publication 61.* Technical Report Publication 68, ICRP.

Kloosterman, J. (1996). *Program Biftox - A Tool to Calculate the Radiotoxicity of a Nuclide Mixture.* Petten, Netherlands: ECN.

Korea Atomic Energy Research Institute. (2000). *Table of Nuclides*. Retrieved June 23, 2014, from http://atom.kaeri.re.kr/

Lung, M., & Gremm, O. (1998). Perspectives of the Thorium Fuel Cycle. *Nuclear Engineering and Design 180*, 133-146.

Massimo, L. (1976). *Physics of High Temperature Reactors.* Exeter, GB: Wheaton en Co.

NEA. (2007). *Radioactive waste management and decommissioning in the Netherlands.* Retrieved May 4, 2014, from Radioactive Waste Management Programmes in OECD/NEA Member Countries: http://www.oecd-nea.org/rwm/profiles/Netherlands_report_web.pdf

Nifenecker, H., Meplan, O., & David, S. (2003). *Accelerator Driven Subcritical Reactors.* Bristol: IoP.

NNL. (2012). *Comparison of Thorium and Uranium Fuel Cycles.* United Kingdom: National Nuclear Laboratory.

NRC. (2002). *Radioactive Waste: Production, Storage, Disposal.* Washington D.C.: U.S. Nuclear Regulatory Commission.

ORNL. (2009). *Scale: A Modelar Code System for Performing Standardized Computer Analyses.*

Ougouag, A.M., Cogliati, J., & Kloosterman, J. (2005). *Methods for Modeling the Packing of Fuel Elements in Pebble Bed Reactors.* Idaho: INL.

Reutler, H., & Lohnert, G. (1984). Adventages of Going Modular in Htrs. *Nuclear Engineering and Design 78*, 129-136.

Sahin, S., Sahin, H., & Acir, A. (2012). Life Hybrid Reactor as Reactor Grade Plutonium Burner. *Energy Conversion and Management 63*, 44-50.

Stone, N. (2000). *Nuclide Table*. Retrieved May 2014, from Table of Nuclear Magnetic Dipole and Electric Quadrupole Moments: http://atom.kaeri.re.kr/ton/nuc7.html

U.S. Department of Energy Office of Environmental Management. (2001). *Depleted Uranium Hexafluoride Fact Sheet*. Retrieved May 28, 2014, from http://web.ead.anl.gov/uranium/pdf/uraniumcharacteristicsfs.pdf

van Dam, H., van der Hagen, T., & Hoogenboom, J. (2005). *Nuclear Reactor Physics.* Delft: Delft University of Technology.

Vandeplassche, D., Biarotte, J., Podlech, H., & Klein, H. (2011). The Myrrha Linear Accelerator.

WNA. (2012). *Uranium Mining Overview*. Retrieved June 24, 2014, from World Nuclear Association: http://www.world-nuclear.org/info/nuclear-fuel-cycle/mining-of-uranium/uranium-mining-overview/

WNA. (2014). *Chernobyl Accident 1986*. Retrieved June 11, 2014, from World Nuclear Association: http://www.world-nuclear.org/info/safety-and-security/safety-of-plants/chernobyl-accident/

WNA. (2014). *Fukushima Accident*. Retrieved June 11, 2014, from World Nuclear Association: http://www.world-nuclear.org/info/safety-and-security/safety-of-plants/fukushima-accident/

Wols, F., Kloosterman, J., & Lathouwers, D. (2012). Fuel Pebble Design Studies of a High Temperature Reactor using Thorium. *Proceedings of the HTR 2012*.

Zhang, Z., Wu, Z., Wang, D., Xu, Y., Sun, Y., & Dong, Y. (2009). Current status and technical description of Chinese 2 x 250 MW_th HTR-PM demonstration plant. *Nuclear Engineering and Design 239*, 2012-2019.

Zheng, Y., Shi, L., & Dong, Y. (2009). Thermohydraulic transient studies of the Chinese 200 MWe HTR-PM for loss of forced cooling accidents. *Annals of Nuclear Energy 36*, 742.

APPENDICES

APPENDIX A: URANIUM PRODUCTION WITH USE OF A LINAC

This appendix shows an energy yield calculation on the production of U-233 with use of a linear accelerator to assess its energetic feasibility. (Vandeplassche, Biarotte, Podlech, & Klein, 2011)

The energy produced out of 1 tonne heavy metal after one burn-up cycle is 90 GWd_{th}, where *th* indicates that this is thermal energy. This has to be converted into electrical energy. The thermal efficiency given for the used PBR design is 42% (Zhang, Wu, Wang, Xu, Sun, & Dong, 2009). This leads to 37.8 GWd_e/907 GWh_e electrical energy out of one tone heavy metal. A conversion to *GWh* is made in order to have more commonly used units.

One tonne of heavy metal contains 6.52 % U-233, which was calculated in the results section in order to gain an equivalent configuration to the HTR-PM. (Zhang, Wu, Wang, Xu, Sun, & Dong, 2009). The simulation of the pebble burn-up without recycling for this configuration (see the results section) shows that the balance between production and consumption of U-233 in one burn-up cycle is only 1.62 % of a tonne HM. This means that after each burn-up cycle 49 kg U-233 has to be added in order to gain the initial configurations.

This 49 kg U-233 can be produced out of Th-232 if this thorium captures a neutron and Th-233 is produced, after two times decay steps forms U-233. (Wols, Kloosterman, & Lathouwers, 2012) The neutrons required to drive this chain reaction have to be produced by the Linac, as described in the theory.

In the best case scenario, every produced neutron will be captured by a thorium atom, this is impossible in practice due to leakage and absorption but for this calculation it is only an assumption that all neutrons will be captured.

The mass of one atom of U-233 is $3.87 \cdot 10^{-25}$ kg. (Korea Atomic Energy Research Institute, 2000). This means that $\frac{49}{3.87 \cdot 10^{-25}} = 1.266 \cdot 10^{26}$ atoms and thus neutrons are needed. The reference Linac needed in this survey is the one used at the Belgium Myrrha project. The neutron yield of this Linac is 15 neutrons per proton accelerated to 600 MeV, which is equal to $2.67 \cdot 10^{-23}$ GWh_e. However, the actual used energy of the Linac will be higher, because not all the energy goes into the acceleration of the protons. The typical efficiency of such a Linac is 30% (Nifenecker, Meplan, & David, 2003) which leads to a required energy per accelerated proton of $8.9 \cdot 10^{-23}$ GWh_e. The yield of 15 neutrons per proton means that $8.44 \cdot 10^{24}$ protons are needed to produce the required U-233. So, in the end this comes down to $8.44 \cdot 10^{24} \cdot 8.9 \cdot 10^{-23} = 751$ GWh_e.

This is almost the entire energy produced by a single burn-up cycle. This makes it rather uneconobicaly to use this method in the recycling scheme. In addition, this was only the best case scenario, leakage and absorption of neutrons were even neglected as mentioned before.

APPENDIX B: DENSITY CALCULATIONS

The simplified method to obtain the density of the different fuels is based on the mainly used compositions of the fuel in the pebbles, namely as an oxide by 2 oxygen molecules for each thorium/uranium molecule. This leads to ThO_2 and UO_2 for case Thorium and Uranium respectively. Table B.1 gives the relevant Isotopes for calculating ρ. (Stone, 2000) and the densities of ThO_2 and UO_2. (Haynes, 2014-2015)

Table B.1: *Molecular masses of the relevant isotopes for calculating ρ*

Isotope	Value	Units
Masses		
Th-232	232.0380504	Amu
U-233	233.0396282	Amu
U-235	235.0439231	Amu
U-238	238.0507826	Amu
O-16	15.9949146	Amu
Densities		
ThO_2	10.0	g/cm³
UO_2	10.96	g/cm³

Using the values in Table B.1 it is possible to calculate the densities used in both case Thorium and Uranium by entering them in formulas (B.1), (B.2), (B.3) and (B.4).

$$\rho_{Th-232} = \frac{M_{Th-232}}{M_{Th-232} + 2 \cdot M_{O-16}} \cdot \rho_{ThO_2} \qquad \text{(B.1)}$$

$$\rho_{U-233} = \frac{M_{U-233}}{M_{U-233} + 2 \cdot M_{O-16}} \cdot \rho_{UO_2} \qquad \text{(B.2)}$$

$$\rho_{U-235} = \frac{M_{U-235}}{M_{U-235} + 2 \cdot M_{O-16}} \cdot \rho_{UO_2} \qquad \text{(B.3)}$$

$$\rho_{U-238} = \frac{M_{U-238}}{M_{U-238} + 2 \cdot M_{O-16}} \cdot \rho_{UO_2} \qquad \text{(B.4)}$$

Table C.2 gives the numerical values of these densities.

Table C.2: *Densities of the different fuel elements*

Isotope	Density	Units
Th-232	8.78	g/cm³
U-233	9.65	g/cm³
U-235	9.66	g/cm³
U-238	9.67	g/cm³

To calculate the total density use is made of formula (B.5) and (B.6).

$$\rho_{Case\,A} = p \cdot \rho_{U-233} + (1-p) \cdot \rho_{Th-232} \qquad \text{(B.5)}$$

$$\rho_{Case\,B} = p \cdot \rho_{U-235} + (1-p) \cdot \rho_{U-238} \qquad \text{(B.6)}$$

These formulas lead to a density of 8.84 [g/cm²] in case Thorium and a density of 9.66 [g/cm²] in case Uranium.

APPENDIX C: DOSE COEFFICIENTS OF NUCLIDES

Table C.1: *Dose coefficients of nuclides (Sv/Bq) as provided in ICRP's Technical Report Publication 68* **(ICRP, 1994)**. *The ratio in the third column is the ratio with the dose coefficients of nuclides provide in ICRP's Technical Report Publication 61* **(ICRP, 1990)**.

Nuclide	Coefficient	Ratio
010030	4.2e-11	2.10
040070	2.8e-11	0.84
040100	1.1e-09	0.55
060110	2.4e-11	7.20
060140	5.8e-10	1.16
090180	4.9e-11	0.98
110220	3.2e-09	1.12
110240	4.3e-10	1.08
120280	2.2e-09	0.88
130260	3.5e-09	0.70
140310	1.6e-10	1.60
140320	5.6e-10	0.56
150320	2.4e-09	0.96
150330	2.4e-10	0.96
160350	7.7e-10	2.69
170360	9.3e-10	0.93
170380	1.2e-10	1.20
170390	8.5e-11	0.85
190400	6.2e-09	1.24
190420	4.3e-10	1.08
190430	2.5e-10	1.13
190440	8.4e-11	0.84
190450	5.4e-11	1.08
200410	2.9e-10	1.01
200450	7.6e-10	0.76
200470	1.6e-09	0.80
210430	1.9e-10	0.95
210440	3.5e-10	1.05
210441	2.4e-09	0.72
210460	1.5e-09	0.75
210470	5.4e-10	0.81
210480	1.7e-09	0.85
210490	8.2e-11	1.23
220440	5.8e-09	0.87
220450	1.5e-10	0.75
230470	6.3e-11	0.94
230480	2.0e-09	0.80
230490	1.8e-11	0.81
240480	2.0e-10	0.80
240490	6.1e-11	1.22
240510	3.8e-11	0.76
250510	9.3e-11	0.93
250520	1.8e-09	0.90
250521	6.9e-11	1.04
250530	3.0e-11	0.90

Nuclide	Coefficient	Ratio
250540	7.1e-10	1.06
250560	2.5e-10	1.13
260520	1.4e-09	0.70
260550	3.3e-10	1.65
260590	1.8e-09	0.90
260600	1.1e-07	2.75
270550	1.1e-09	1.10
270560	2.5e-09	0.75
270570	2.1e-10	0.63
270580	7.4e-10	0.74
270581	2.4e-11	0.96
270600	3.4e-09	0.51
270601	1.7e-12	0.85
270610	7.4e-11	1.11
270621	4.7e-11	0.94
280560	8.6e-10	0.86
280570	8.7e-10	0.87
280590	6.3e-11	0.94
280630	1.5e-10	0.75
280650	1.8e-10	0.90
280660	3.0e-09	0.75
290600	7.0e-11	1.05
290610	1.2e-10	1.20
290640	1.2e-10	1.20
290670	3.4e-10	0.85
300620	9.4e-10	0.94
300630	7.9e-11	1.19
300650	3.9e-09	0.97
300690	3.1e-11	1.09
300691	3.3e-10	0.82
300711	2.4e-10	1.08
300720	1.4e-09	0.70
310650	3.7e-11	1.11
310660	1.2e-09	1.20
310670	1.9e-10	0.76
310680	1.0e-10	1.00
310700	3.1e-11	1.09
310720	1.1e-09	1.10
310730	2.6e-10	1.04
320660	1.0e-10	1.50
320670	6.5e-11	0.98
320680	1.3e-09	4.55
320690	2.4e-10	2.40
320710	1.2e-11	4.80
320750	4.6e-11	1.15
320770	3.3e-10	1.65
320780	1.2e-10	1.20
330690	5.7e-11	1.14
330700	1.3e-10	1.30
330710	4.6e-10	0.92
330720	1.8e-09	0.90
330730	2.6e-10	1.04
330740	1.3e-09	1.30
330760	1.6e-09	0.80
330770	4.0e-10	1.00
330780	2.1e-10	1.05
340700	1.4e-10	1.40
340730	3.9e-10	0.98

Nuclide	Coefficient	Ratio
340731	4.1e-11	1.02
340750	2.6e-09	1.17
340790	2.9e-09	1.45
340810	2.7e-11	1.08
340811	5.9e-11	1.18
340830	5.1e-11	1.02
350740	8.4e-11	0.84
350741	1.4e-10	0.70
350750	7.9e-11	1.19
350760	4.6e-10	1.15
350770	9.6e-11	0.96
350800	3.1e-11	1.09
350801	1.1e-10	1.10
350820	5.4e-10	1.08
350830	4.3e-11	1.07
350840	8.8e-11	0.88
370790	5.0e-11	1.00
370810	5.4e-11	1.08
370811	9.7e-12	0.97
370821	1.3e-10	1.30
370830	1.9e-09	0.95
370840	2.8e-09	1.12
370860	2.8e-09	1.12
370870	1.5e-09	1.50
370880	9.0e-11	0.90
370890	4.7e-11	0.94
380800	3.5e-10	1.23
380810	7.8e-11	1.17
380820	6.1e-09	0.61
380830	5.8e-10	0.87
380850	5.6e-10	1.12
380851	6.1e-12	1.22
380871	3.3e-11	1.15
380890	2.6e-09	0.78
380900	2.8e-08	0.84
380910	7.6e-10	1.14
380920	4.9e-10	0.98
390860	9.6e-10	0.96
390861	5.6e-11	0.84
390870	5.5e-10	0.82
390880	1.3e-09	0.65
390900	2.7e-09	0.68
390901	1.7e-10	0.77
390910	2.4e-09	0.60
390911	1.1e-11	1.10
390920	4.9e-10	0.98
390930	1.2e-09	1.20
390940	8.1e-11	1.22
390950	4.6e-11	0.92
400860	8.6e-10	0.86
400880	3.3e-10	0.82
400890	7.9e-10	0.79
400930	2.8e-10	0.98
400950	8.8e-10	0.88
400970	2.1e-09	0.84
410880	6.3e-11	1.58
410890	3.0e-10	1.20
410891	1.4e-10	1.40

Nuclide	Coefficient	Ratio
410900	1.2e-09	0.60
410931	1.2e-10	0.60
410940	1.7e-09	0.77
410950	5.8e-10	0.87
410951	5.6e-10	0.56
410960	1.1e-09	1.10
410970	6.8e-11	1.36
410980	1.1e-10	1.10
420900	6.2e-10	0.93
420930	2.6e-09	10.40
420931	2.8e-10	0.98
420990	1.2e-09	0.60
430930	4.9e-11	1.23
430931	2.4e-11	1.08
430940	1.8e-10	0.90
430941	1.1e-10	1.10
430950	1.6e-10	0.80
430951	6.2e-10	1.24
430960	1.1e-09	1.10
430961	1.3e-11	1.30
430970	8.3e-11	1.25
430971	6.6e-10	1.32
430980	2.3e-09	1.15
430990	7.8e-10	1.17
430991	2.2e-11	1.10
431010	1.9e-11	0.95
431040	8.1e-11	1.22
440940	9.4e-11	1.41
440970	1.5e-10	0.75
441030	7.3e-10	0.73
441050	2.6e-10	0.91
441060	7.0e-09	0.70
450990	5.1e-10	0.76
450991	6.6e-11	0.99
451000	7.1e-10	1.06
451010	5.5e-10	0.82
451011	2.2e-10	0.77
451020	2.6e-09	0.91
451021	1.2e-09	0.60
451031	3.8e-12	1.14
451050	3.7e-10	0.74
451061	1.6e-10	0.80
451070	2.4e-11	1.08
461000	9.4e-10	0.94
461010	9.4e-11	0.94
461030	1.9e-10	0.67
461070	3.7e-11	0.56
461090	5.5e-10	0.82
471020	4.0e-11	1.00
471030	4.3e-11	1.07
471040	6.0e-11	1.20
471041	5.4e-11	1.08
471050	4.7e-10	0.94
471060	3.2e-11	1.12
471061	1.5e-09	0.75
471081	2.3e-09	1.15
471101	2.8e-09	0.98
471110	1.3e-09	0.65

Nuclide	Coefficient	Ratio
471120	4.3e-10	1.08
471150	6.0e-11	0.90
481040	5.8e-11	1.16
481070	6.2e-11	0.93
481090	2.0e-09	0.90
481130	2.5e-08	1.00
481131	2.3e-08	1.04
481150	1.4e-09	0.70
481151	3.3e-09	0.82
481170	2.8e-10	1.12
481171	2.8e-10	0.98
491090	6.6e-11	0.99
491100	1.0e-10	1.00
491101	2.4e-10	1.08
491110	2.9e-10	0.73
491120	1.0e-11	1.00
491131	2.8e-11	1.26
491141	4.1e-09	0.62
491150	3.2e-08	0.96
491151	8.6e-11	0.86
491161	6.4e-11	1.28
491170	3.1e-11	1.09
491171	1.2e-10	1.20
491191	4.7e-11	0.94
501100	3.5e-10	1.05
501110	2.3e-11	1.04
501130	7.3e-10	0.73
501171	7.1e-10	0.71
501191	3.4e-10	0.68
501210	2.3e-10	0.81
501211	3.8e-10	0.57
501230	2.1e-09	0.63
501231	3.8e-11	1.14
501250	3.1e-09	0.62
501260	4.7e-09	0.71
501270	2.0e-10	1.00
501280	1.5e-10	1.50
511150	2.4e-11	1.08
511160	2.6e-11	1.04
511161	6.7e-11	1.01
511170	1.8e-11	0.90
511181	2.1e-10	0.94
511190	8.1e-11	0.81
511201	1.2e-09	0.60
511200	1.4e-11	0.70
511220	1.7e-09	0.68
511240	2.5e-09	0.75
511241	8.0e-12	1.20
511250	1.1e-09	1.10
511260	2.4e-09	0.72
511261	3.6e-11	1.08
511270	1.7e-09	0.68
511280	7.6e-10	0.76
511281	3.3e-11	1.48
511290	4.2e-10	1.05
511300	9.1e-11	0.91
511310	1.0e-10	1.00
521160	1.7e-10	0.85

Nuclide	Coefficient	Ratio
521210	4.3e-10	1.08
521211	2.3e-09	1.15
521230	4.4e-09	6.60
521231	1.4e-09	1.40
521251	8.7e-10	0.87
521270	1.7e-10	0.85
521271	2.3e-09	1.04
521290	6.3e-11	1.26
521291	3.0e-09	0.75
521310	8.7e-11	0.26
521311	1.9e-09	0.57
521320	3.7e-09	0.93
521330	7.2e-11	1.08
521331	2.8e-10	0.98
521340	1.1e-10	1.10
531200	3.4e-10	1.02
531201	2.1e-10	0.94
531210	8.2e-11	0.82
531230	2.1e-10	0.94
531240	1.3e-08	0.65
531250	1.5e-08	0.75
531260	2.9e-08	0.87
531280	4.6e-11	0.92
531290	1.1e-07	1.10
531300	2.0e-09	1.00
531310	2.2e-08	0.88
531320	2.9e-10	1.01
531321	2.2e-10	0.99
531330	4.3e-09	0.86
531340	1.1e-10	1.10
531350	9.3e-10	0.93
551250	3.5e-11	1.05
551270	2.4e-11	0.96
551290	6.0e-11	0.90
551300	2.8e-11	0.98
551310	5.8e-11	0.87
551320	5.0e-10	1.00
551340	1.9e-08	0.95
551341	2.0e-11	1.00
551350	2.0e-09	1.00
551351	1.9e-11	0.95
551360	3.0e-09	1.05
551370	1.3e-08	0.65
551380	9.2e-11	0.92
561260	2.6e-10	1.30
561280	2.7e-09	0.81
561310	4.5e-10	0.90
561311	4.9e-12	0.98
561330	1.0e-09	1.00
561331	5.5e-10	0.82
561351	4.5e-10	0.90
561390	1.2e-10	1.20
561400	2.5e-09	0.75
561410	7.0e-11	1.05
561420	3.5e-11	1.23
571310	3.5e-11	1.23
571320	3.9e-10	0.98
571350	3.0e-11	0.90

Nuclide	Coefficient	Ratio
571370	8.1e-11	0.81
571380	1.1e-09	0.55
571400	2.0e-09	0.80
571410	3.6e-10	1.08
571420	1.8e-10	0.90
571430	5.6e-11	0.84
581340	2.5e-09	0.75
581350	7.9e-10	0.79
581370	2.5e-11	0.88
581371	5.4e-10	0.81
581390	2.6e-10	0.65
581410	7.1e-10	0.71
581430	1.1e-09	0.55
581440	5.2e-09	0.52
591360	3.3e-11	0.99
591370	4.0e-11	1.20
591381	1.3e-10	1.30
591390	3.1e-11	0.93
591420	1.3e-09	0.65
591421	1.7e-11	0.85
591430	1.2e-09	0.60
591440	5.0e-11	1.00
591450	3.9e-10	0.98
591470	3.3e-11	0.99
601360	9.9e-11	0.99
601380	6.4e-10	0.96
601390	2.0e-11	1.00
601391	2.5e-10	1.00
601410	8.3e-12	1.25
601470	1.1e-09	0.55
601490	1.2e-10	0.60
601510	3.0e-11	0.90
611410	3.6e-11	1.08
611430	2.3e-10	0.81
611440	9.7e-10	0.97
611450	1.1e-10	0.55
611460	9.0e-10	0.90
611470	2.6e-10	0.65
611480	2.7e-09	0.68
611481	1.8e-09	0.81
611490	9.9e-10	0.50
611500	2.6e-10	1.04
611510	7.3e-10	0.73
621410	3.9e-11	0.98
621411	6.5e-11	0.98
621420	1.9e-10	0.95
621450	2.1e-10	0.74
621460	5.4e-08	1.62
621470	4.9e-08	1.47
621510	9.8e-11	0.49
621530	7.4e-10	0.74
621550	2.9e-11	1.02
621560	2.5e-10	0.88
631450	7.5e-10	0.75
631460	1.3e-09	0.65
631470	4.4e-10	0.66
631480	1.3e-09	0.65
631490	1.0e-10	0.50

Nuclide	Coefficient	Ratio
631500	1.3e-09	0.65
631520	1.4e-09	0.70
631521	5.0e-10	1.00
631540	2.0e-09	0.70
631550	3.2e-10	0.64
631560	2.2e-09	0.66
631570	6.0e-10	0.90
631580	9.4e-11	0.94
641450	4.4e-11	1.10
641460	9.6e-10	0.48
641470	6.1e-10	0.92
641480	5.5e-08	1.65
641490	4.5e-10	0.68
641510	2.0e-10	0.70
641520	4.1e-08	1.64
641530	2.7e-10	0.68
641590	4.9e-10	0.73
651470	1.6e-10	0.80
651490	2.5e-10	1.00
651500	2.5e-10	1.00
651510	3.4e-10	0.85
651530	2.5e-10	0.75
651540	6.5e-10	0.98
651550	2.1e-10	0.74
651560	1.2e-09	0.60
651562	1.7e-10	0.68
651561	8.1e-11	0.81
651570	3.4e-11	0.85
651580	1.1e-09	0.55
651600	1.6e-09	0.07
651610	7.2e-10	0.72
661550	1.3e-10	0.65
661570	6.1e-11	0.91
661590	1.0e-10	0.50
661650	1.1e-10	1.10
661660	1.6e-09	0.56
671550	3.7e-11	1.11
671570	6.5e-12	0.98
671590	7.9e-12	1.19
671610	1.3e-11	1.30
671620	3.3e-12	0.99
671621	2.6e-11	1.17
671640	9.5e-12	0.95
671641	1.6e-11	0.80
671660	1.4e-09	0.70
671661	2.0e-09	0.90
671670	8.3e-11	1.25
681610	8.0e-11	1.20
681650	1.9e-11	0.85
681690	3.7e-10	0.56
681710	3.6e-10	0.90
681720	1.0e-09	0.50
691620	2.9e-11	1.02
691660	2.8e-10	0.98
691670	5.6e-10	0.56
691700	1.3e-09	0.65
691710	1.1e-10	0.55
691720	1.7e-09	0.68

Nuclide	Coefficient	Ratio
691730	3.1e-10	0.93
691750	2.7e-11	0.94
701620	2.3e-11	1.15
701660	9.5e-10	0.95
701670	6.7e-12	1.00
701690	7.1e-10	0.71
701750	4.4e-10	0.66
701770	9.7e-11	0.97
701780	1.2e-10	1.20
711690	4.6e-10	0.92
711700	9.9e-10	0.99
711710	6.7e-10	0.67
711720	1.3e-09	0.65
711730	2.6e-10	0.78
711740	2.7e-10	0.68
711741	5.3e-10	0.79
711760	1.8e-09	0.72
711761	1.7e-10	0.85
711770	5.3e-10	0.53
711771	1.7e-09	0.68
711780	4.7e-11	0.94
711781	3.8e-11	0.95
711790	2.1e-10	1.05
721700	4.8e-10	0.72
721720	1.0e-09	0.50
721730	2.3e-10	0.92
721750	4.1e-10	0.82
721771	8.1e-11	1.22
721781	4.7e-09	0.94
721791	1.2e-09	0.60
721801	1.7e-10	0.85
721810	1.1e-09	0.55
721820	3.0e-09	1.05
721821	4.2e-11	1.05
721830	7.3e-11	1.10
721840	5.2e-10	1.04
731720	5.3e-11	1.06
731730	1.9e-10	0.95
731740	5.7e-11	1.14
731750	2.1e-10	0.94
731760	3.1e-10	0.93
731770	1.1e-10	0.55
731780	7.8e-11	1.17
731790	6.5e-11	0.65
731800	8.4e-10	0.84
731801	5.4e-11	0.81
731820	1.5e-09	0.68
731821	1.2e-11	1.20
731830	1.3e-09	0.65
731840	6.8e-10	1.02
731850	6.8e-11	1.02
731860	3.3e-11	0.99
741760	1.1e-10	1.10
741770	6.1e-11	0.91
741780	2.5e-10	0.75
741790	3.3e-12	1.15
741810	8.2e-11	0.82
741850	5.0e-10	0.75

Nuclide	Coefficient	Ratio
741870	7.1e-10	0.71
741880	2.3e-09	0.57
751770	2.2e-11	1.10
751780	2.5e-11	1.00
751810	4.2e-10	1.05
751820	1.4e-09	1.40
751821	2.7e-10	1.08
751840	1.0e-09	1.50
751841	1.5e-09	1.50
751860	1.5e-09	1.50
751861	2.2e-09	1.10
751870	5.1e-12	1.27
751880	1.4e-09	1.40
751881	3.0e-11	1.05
751890	7.8e-10	1.17
761800	1.7e-11	0.85
761810	8.9e-11	0.89
761820	5.6e-10	0.84
761850	5.1e-10	0.76
761891	1.8e-11	0.90
761910	5.7e-10	0.57
761911	9.6e-11	0.96
761930	8.1e-10	0.81
761940	2.4e-09	0.60
771820	4.8e-11	0.96
771840	1.7e-10	0.85
771850	2.6e-10	0.91
771860	4.9e-10	0.98
771870	1.2e-10	1.20
771880	6.3e-10	0.94
771890	2.4e-10	0.60
771900	1.2e-09	0.60
771901	8.0e-12	0.80
771920	1.4e-09	0.70
771921	3.1e-10	0.93
771940	1.3e-09	0.65
771941	2.1e-09	0.73
771950	1.0e-10	1.00
771951	2.1e-10	1.05
781860	9.3e-11	0.93
781880	7.6e-10	0.76
781890	1.2e-10	1.20
781910	3.4e-10	0.85
781930	3.1e-11	0.62
781931	4.5e-10	0.68
781951	6.3e-10	0.63
781970	4.0e-10	0.80
781971	8.4e-11	0.84
781990	3.9e-11	0.98
782000	1.2e-09	0.60
791930	1.3e-10	0.65
791940	4.2e-10	0.84
791950	2.5e-10	0.63
791980	1.0e-09	0.50
791981	1.3e-09	0.65
791990	4.4e-10	0.66
792000	6.8e-11	1.02
792001	1.1e-09	1.10

Nuclide	Coefficient	Ratio
792010	2.4e-11	1.08
801930	8.2e-11	0.82
801931	4.0e-10	0.80
801940	5.1e-08	1.02
801950	9.7e-11	0.97
801951	5.6e-10	0.84
801970	2.3e-10	0.69
801971	4.7e-10	0.70
801991	3.1e-11	1.09
802030	1.9e-09	0.95
811940	8.1e-12	1.22
811941	4.0e-11	1.00
811950	2.7e-11	1.08
811970	2.3e-11	1.15
811980	7.3e-11	1.10
811981	5.4e-11	1.08
811990	2.6e-11	1.04
812000	2.0e-10	1.00
812010	9.5e-11	1.43
812020	4.5e-10	1.13
812040	1.3e-09	1.95
821951	2.9e-11	1.02
821980	1.0e-10	2.50
821990	5.4e-11	1.08
822000	4.0e-10	0.80
822010	1.6e-10	0.80
822020	8.7e-09	0.87
822021	1.3e-10	1.30
822030	2.4e-10	0.72
822050	2.8e-10	0.84
822090	5.7e-11	1.14
822100	6.8e-07	0.68
822110	1.8e-10	0.90
822120	5.9e-09	0.59
822140	1.4e-10	0.70
832000	5.1e-11	1.02
832010	1.2e-10	1.20
832020	8.9e-11	0.89
832030	4.8e-10	0.96
832050	9.0e-10	0.90
832060	1.9e-09	0.85
832070	1.3e-09	0.65
832100	1.3e-09	0.65
832101	1.5e-08	0.75
832120	2.6e-10	1.17
832130	2.0e-10	1.00
832140	1.1e-10	1.10
842030	5.2e-11	1.04
842050	5.9e-11	1.18
842070	1.4e-10	0.70
842100	2.4e-07	1.08
852070	2.3e-10	0.92
852110	1.1e-08	1.10
872220	7.1e-10	1.06
872230	2.3e-09	1.04
882230	1.0e-07	1.00
882240	6.5e-08	0.98
882250	9.5e-08	1.43

Nuclide	Coefficient	Ratio
882260	2.8e-07	1.26
882270	8.4e-11	1.68
882280	6.7e-07	2.35
892240	7.0e-10	0.70
892250	2.4e-08	0.60
892260	1.0e-08	0.50
892270	1.1e-06	0.50
892280	4.3e-10	0.86
902260	3.6e-10	1.08
902270	8.9e-09	0.89
902280	7.0e-08	1.05
902290	4.8e-07	0.96
902300	2.1e-07	3.15
902310	3.4e-10	0.85
902320	2.2e-07	0.55
902340	3.4e-09	0.68
912280	7.8e-10	0.78
912300	9.2e-10	0.46
912310	7.1e-07	0.36
912320	7.2e-10	0.72
912330	8.7e-10	0.87
912340	5.1e-10	1.02
922300	5.5e-08	0.55
922310	2.8e-10	0.70
922320	3.3e-07	3.30
922330	5.0e-08	1.75
922340	4.9e-08	1.72
922350	4.6e-08	1.61
922360	4.6e-08	1.61
922370	7.7e-10	0.77
922380	4.4e-08	1.76
922390	2.8e-11	0.98
922400	1.1e-09	1.10
932320	9.7e-12	0.97
932330	2.2e-12	1.10
932340	8.1e-10	1.22
932350	5.3e-11	0.53
932360	1.7e-08	0.17
932361	1.9e-10	0.57
932370	1.1e-07	0.17
932380	9.1e-10	0.91
932390	8.0e-10	0.80
932400	8.2e-11	1.23
942340	1.6e-10	0.80
942350	2.1e-12	1.05
942360	8.6e-08	0.43
942370	1.0e-10	0.50
942380	2.3e-07	0.46
942390	2.5e-07	0.50
942400	2.5e-07	0.50
942410	4.7e-09	0.47
942420	2.4e-07	0.48
942430	8.5e-11	0.85
942440	2.4e-07	0.48
942450	7.2e-10	1.08
942460	3.3e-09	0.66
952370	1.8e-11	0.90
952380	3.2e-11	1.12

Nuclide	Coefficient	Ratio
952390	2.4e-10	0.96
952400	5.8e-10	0.87
952410	2.0e-07	0.30
952420	3.0e-10	0.75
952421	1.9e-07	0.38
952430	2.0e-07	0.30
952440	4.6e-10	0.92
952441	2.9e-11	1.02
952450	6.2e-11	1.55
952460	5.8e-11	1.16
952461	3.4e-11	1.02
962380	8.0e-11	1.20
962400	7.6e-09	0.38
962410	9.1e-10	0.46
962420	1.2e-08	0.54
962430	1.5e-07	0.38
962440	1.2e-07	0.36
962450	2.1e-07	0.31
962460	2.1e-07	0.31
962470	1.9e-07	0.38
962480	7.7e-07	0.35
962490	3.1e-11	1.24
962500	4.4e-06	0.44
972450	5.7e-10	0.57
972460	4.8e-10	0.96
972470	3.5e-07	0.52
972490	9.7e-10	0.48
972500	1.4e-10	1.40
982440	7.0e-11	1.05
982460	3.3e-09	0.66
982480	2.8e-08	0.56
982490	3.5e-07	0.52
982500	1.6e-07	0.48
982510	3.6e-07	0.54
982520	9.0e-08	0.45
982530	1.4e-09	0.49
982540	4.0e-07	0.60

APPENDIX D: DOSE TABLES AND PLOTS OF NUCLIDES AND DAUGHTERS

Table D.1: *Radiotoxicity per mole for the most important actinides and their daughter products (Sv/mole) based on* **(ICRP, 1994)** *and calculated with use of the BIFTOX program by J.L. Kloosterman* **(Kloosterman, 1996)**

	Storage time (a)							
Nuclide	**1.0E+01**	**2.0E+01**	**5.0E+01**	**1.0E+02**	**2.0E+02**	**5.0E+02**	**1.0E+03**	**2.0E+03**
902300	3.71E+04	3.76E+04	3.96E+04	4.37E+04	5.22E+04	7.76E+04	1.10E+05	1.57E+05
902320	7.24E-01	8.97E-01	9.69E-01	9.71E-01	9.71E-01	9.71E-01	9.71E-01	9.71E-01
912310	4.20E+05	5.16E+05	6.75E+05	7.53E+05	7.71E+05	7.67E+05	7.59E+05	7.43E+05
912330	4.20E+03	4.25E+03	4.39E+03	4.62E+03	5.08E+03	6.44E+03	8.61E+03	1.26E+04
922320	8.08E+07	7.38E+07	5.48E+07	3.34E+07	1.24E+07	6.28E+05	4.38E+03	2.13E-01
922330	4.20E+03	4.25E+03	4.39E+03	4.62E+03	5.08E+03	6.44E+03	8.61E+03	1.26E+04
922340	2.64E+03	2.64E+03	2.64E+03	2.65E+03	2.66E+03	2.72E+03	2.85E+03	3.22E+03
922350	8.74E-01	8.79E-01	8.97E-01	9.33E-01	1.01E+00	1.25E+00	1.63E+00	2.37E+00
922360	2.60E+01	2.60E+01	2.60E+01	2.60E+01	2.60E+01	2.60E+01	2.60E+01	2.60E+01
922370	6.85E+02	6.85E+02	6.85E+02	6.85E+02	6.86E+02	6.86E+02	6.87E+02	6.90E+02
922380	1.40E-01	1.40E-01	1.40E-01	1.40E-01	1.40E-01	1.41E-01	1.41E-01	1.41E-01
932370	6.85E+02	6.85E+02	6.85E+02	6.85E+02	6.86E+02	6.86E+02	6.87E+02	6.90E+02
932380	3.21E+07	2.96E+07	2.34E+07	1.57E+07	7.14E+06	6.69E+05	1.56E+04	3.17E+03
932390	1.37E+05	1.37E+05	1.37E+05	1.37E+05	1.36E+05	1.35E+05	1.33E+05	1.29E+05
942380	3.21E+07	2.96E+07	2.34E+07	1.57E+07	7.14E+06	6.69E+05	1.56E+04	3.17E+03
942390	1.37E+05	1.37E+05	1.31E+05	1.37E+05	1.36E+05	1.35E+05	1.33E+05	1.29E+05
942400	5.03E+05	5.03E+05	5.01E+05	4.99E+05	4.93E+05	4.78E+05	4.53E+05	4.08E+05
942410	4.98E+06	5.36E+06	5.66E+06	5.37E+06	4.59E+06	2.84E+06	1.27E+06	2.51E+05
942420	8.50E+03	8.50E+03	8.50E+03	8.50E+03	8.50E+03	8.49E+03	8.48E+03	8.41E+03
942430	3.60E+05	3.60E+05	3.60E+05	3.59E+05	3.56E+05	3.50E+05	3.40E+05	3.22E+05
942440	3.99E+01	4.00E+01	4.01E+01	4.03E+01	4.07E+01	4.20E+01	4.40E+01	4.71E+01
952410	6.02E+06	5.92E+06	5.64E+06	5.21E+06	4.44E+06	2.74E+06	1.23E+06	2.49E+05
952421	1.91E+07	1.94E+07	1.98E+07	1.89E+07	1.50E+07	4.75E+06	4.70E+05	6.10E+03
952420	2.68E+07	2.47E+07	1.95E+07	1.31E+07	5.96E+06	5.60E+05	1.45E+04	4.10E+03
952430	3.60E+05	3.60E+05	3.60E+05	3.59E+05	3.56E+05	3.50E+05	3.40E+05	3.22E+05
962420	3.22E+07	2.98E+07	2.35E+07	1.58E+07	7.18E+06	6.73E+05	1.57E+04	3.17E+03
962430	5.25E+07	4.17E+07	2.09E+07	6.68E+06	7.86E+05	1.36E+05	1.34E+05	1.30E+05
962440	6.00E+07	4.10E+07	1.34E+07	2.39E+06	5.36E+05	4.79E+05	4.55E+05	4.09E+05
962450	3.30E+05	3.34E+05	3.47E+05	3.68E+05	4.06E+05	4.82E+05	5.39E+05	5.46E+05
962460	5.86E+05	5.86E+05	5.83E+05	5.79E+05	5.11E+05	5.46E+05	5.08E+05	4.40E+05
962470	1.57E+02	1.57E+02	1.58E+02	1.59E+02	1.60E+02	1.65E+02	1.72E+02	1.87E+02
962480	3.00E+04	3.00E+04	3.00E+04	2.99E+04	2.99E+04	2.99E+04	2.99E+04	2.98E+04
972490	1.30E+07	1.27E+07	1.20E+07	1.09E+07	9.03E+06	5.19E+06	2.26E+06	7.88E+05
982490	1.29E+07	1.27E+07	1.20E+07	1.09E+07	9.01E+06	5.18E+06	2.26E+06	7.87E+05
982500	9.55E+07	5.64E+07	1.20E+07	1.38E+06	5.76E+05	5.47E+05	5.09E+05	4.41E+05
982510	5.26E+06	5.22E+06	5.10E+06	4.91E+06	4.54E+06	3.60E+06	2.45E+06	1.13E+06
982520	3.28E+07	2.41E+06	2.99E+04	2.90E+04	2.90E+04	2.90E+04	2.90E+04	2.89E+04
982530	1.47E+07	1.44E+07	1.36E+07	1.23E+07	1.02E+07	5.88E+06	2.56E+06	8.92E+05
992530	1.39E+07	1.36E+07	1.28E+07	1.17E+07	9.64E+06	5.55E+06	2.42E+06	8.41E+05

	Storage time (a)						
Nuclide	**5.0E+03**	**1.0E+04**	**2.0E+04**	**5.0E+04**	**1.0E+05**	**2.0E+05**	**5.0E+05**
902300	2.60E+01	2.60E+01	2.60E+01	2.59E+01	2.59E+01	2.58E+01	2.56E+01
902320	7.07E+02	7.52E+02	8.78E+02	1.31E+03	1.94E+03	2.93E+03	3.81E+03
912310	1.43E-01	1.48E-01	1.65E-01	2.71E-01	5.47E-01	1.25E+00	2.98E+00
912330	7.07E+02	7.52E+02	8.78E+02	1.31E+03	1.94E+03	2.93E+03	3.81E+03
922320	4.75E+03	7.83E+03	1.37E+04	2.84E+04	4.12E+04	4.67E+04	2.63E+04
922330	1.19E+05	1.03E+05	7.72E+04	3.26E+04	7.76E+03	4.72E+02	3.70E+01
922340	4.75E+03	7.83E+03	1.37E+04	2.84E+04	4.12E+04	4.67E+04	2.63E+04
922350	1.19E+05	1.03E+05	7.72E+04	3.26E+04	7.76E+03	4.72E+02	3.70E+01
922360	2.97E+05	1.75E+05	6.10E+04	2.59E+03	3.90E+01	2.58E+01	2.56E+01
922370	2.80E+03	7.46E+02	8.69E+02	1.30E+03	1.94E+03	2.93E+03	3.80E+03
922380	8.42E+03	8.34E+03	8.19E+03	7.75E+03	7.06E+03	5.86E+03	3.36E+03
932370	2.73E+05	2.12E+05	1.36E+05	4.84E+04	1.12E+04	6.63E+02	3.70E+01
932380	5.68E+01	6.68E+01	7.62E+01	8.09E+01	8.11E+01	8.11E+01	8.09E+01
932390	2.73E+03	7.46E+02	8.69E+02	1.30E+03	1.94E+03	2.93E+03	3.80E+03
942380	5.28E+03	7.82E+03	1.27E+04	2.48E+04	3.53E+04	3.97E+04	2.24E+04
942390	5.40E+03	7.95E+03	1.28E+04	2.49E+04	3.55E+04	3.98E+04	2.25E+04
942400	2.73E+05	2.12E+05	1.36E+05	4.84E+04	1.12E+04	6.63E+02	3.70E+01
942410	4.75E+03	7.83E+03	1.37E+04	2.84E+04	4.12E+04	4.67E+04	2.63E+04
942420	1.19E+05	1.03E+05	7.74E+04	3.27E+04	7.18E+03	4.73E+02	3.70E+01
942430	2.98E+05	1.76E+05	6.11E+04	2.60E+03	3.90E+01	2.58E+01	2.56E+01
942440	4.39E+05	2.86E+05	1.21E+05	1.21E+04	1.98E+03	2.84E+03	3.79E+03
952410	2.87E+05	1.42E+05	3.92E+04	8.22E+03	7.15E+03	5.94E+03	3.40E+03
952421	2.25E+02	2.77E+02	3.51E+02	4.58E+02	5.11E+02	5.09E+02	5.19E+02
952420	2.97E+04	2.94E+04	2.88E+04	2.71E+04	2.44E+04	1.99E+04	1.09E+04
952430	4.58E+05	2.99E+05	1.32E+05	1.25E+04	1.98E+03	2.83E+03	3.79E+03
962420	4.58E+05	2.98E+05	1.32E+05	1.25E+04	1.98E+03	2.83E+03	3.79E+03
962430	2.87E+05	1.42E+05	3.92E+04	8.22E+03	7.14E+03	5.93E+03	3.40E+03
962440	1.12E+05	2.62E+03	3.44E+02	4.55E+02	5.11E+02	5.09E+02	5.19E+02
962450	2.87E+04	2.84E+04	2.79E+04	2.62E+04	2.37E+04	1.93E+04	1.05E+04
962460	5.18E+05	3.38E+05	1.50E+05	1.42E+04	2.24E+03	3.21E+03	4.28E+03
962470	4.90E+05	3.19E+05	1.42E+05	1.34E+04	2.11E+03	3.03E+03	4.05E+03
962480	2.60E+01	2.60E+01	2.60E+01	2.59E+01	2.59E+01	2.58E+01	2.56E+01
972490	7.07E+02	7.52E+02	8.78E+02	1.31E+03	1.94E+03	2.93E+03	3.81E+03
982490	1.43E-01	1.48E-01	1.65E-01	2.71E-01	5.47E-01	1.25E+00	2.98E+00
982500	7.07E+02	7.52E+02	8.78E+02	1.31E+03	1.94E+03	2.93E+03	3.81E+03
982510	4.75E+03	7.83E+03	1.37E+04	2.84E+04	4.12E+04	4.67E+04	2.63E+04
982520	1.19E+05	1.03E+05	7.72E+04	3.26E+04	7.76E+03	4.72E+02	3.70E+01
982530	4.75E+03	7.83E+03	1.37E+04	2.84E+04	4.12E+04	4.67E+04	2.63E+04
992530	1.19E+05	1.03E+05	7.72E+04	3.26E+04	7.76E+03	4.72E+02	3.70E+01

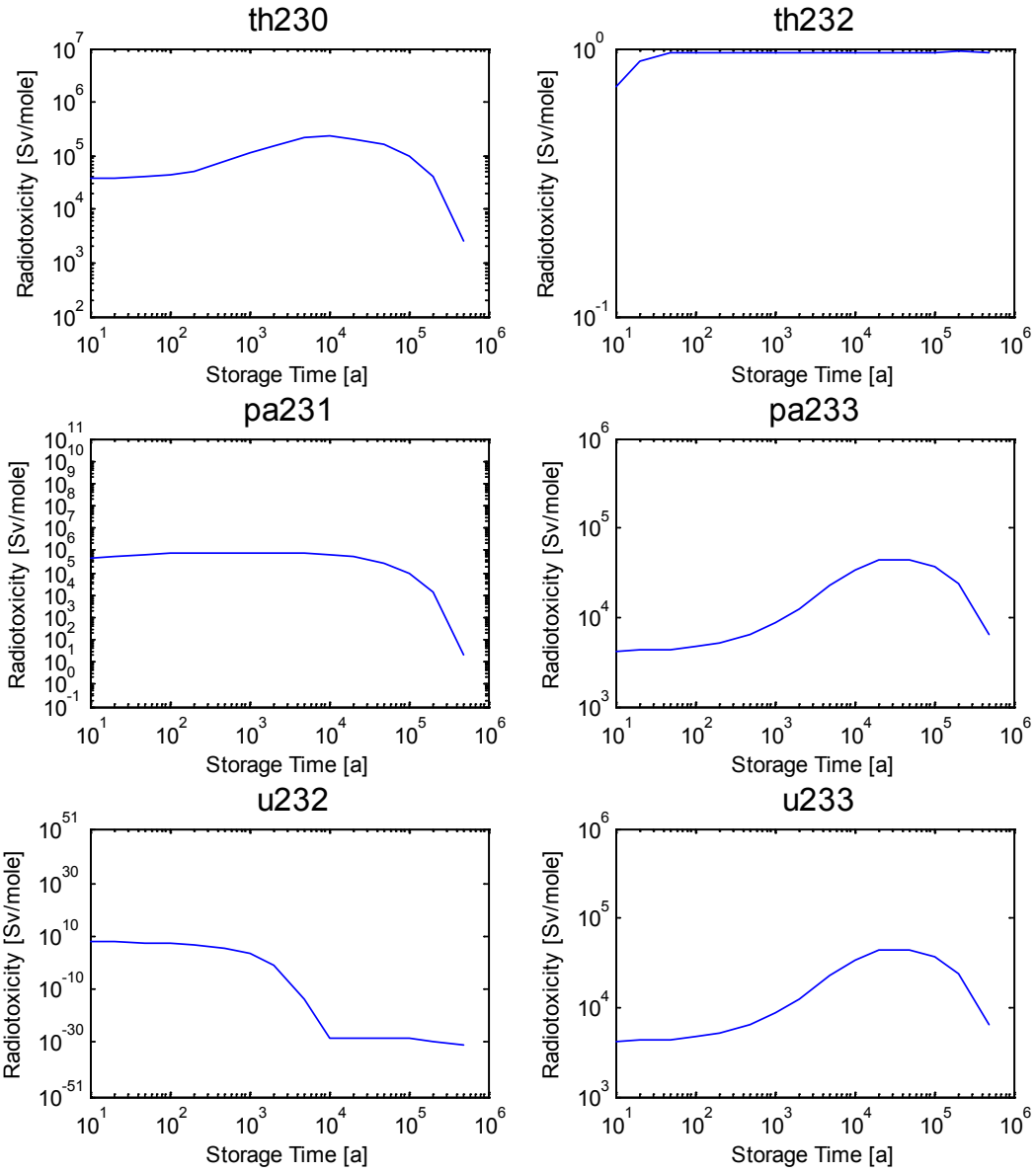

Figure D.1: *Radiotoxicity of Th-230, Th-232, Pa-231, Pa-233, U-232 and U-233 and all their daughters.*

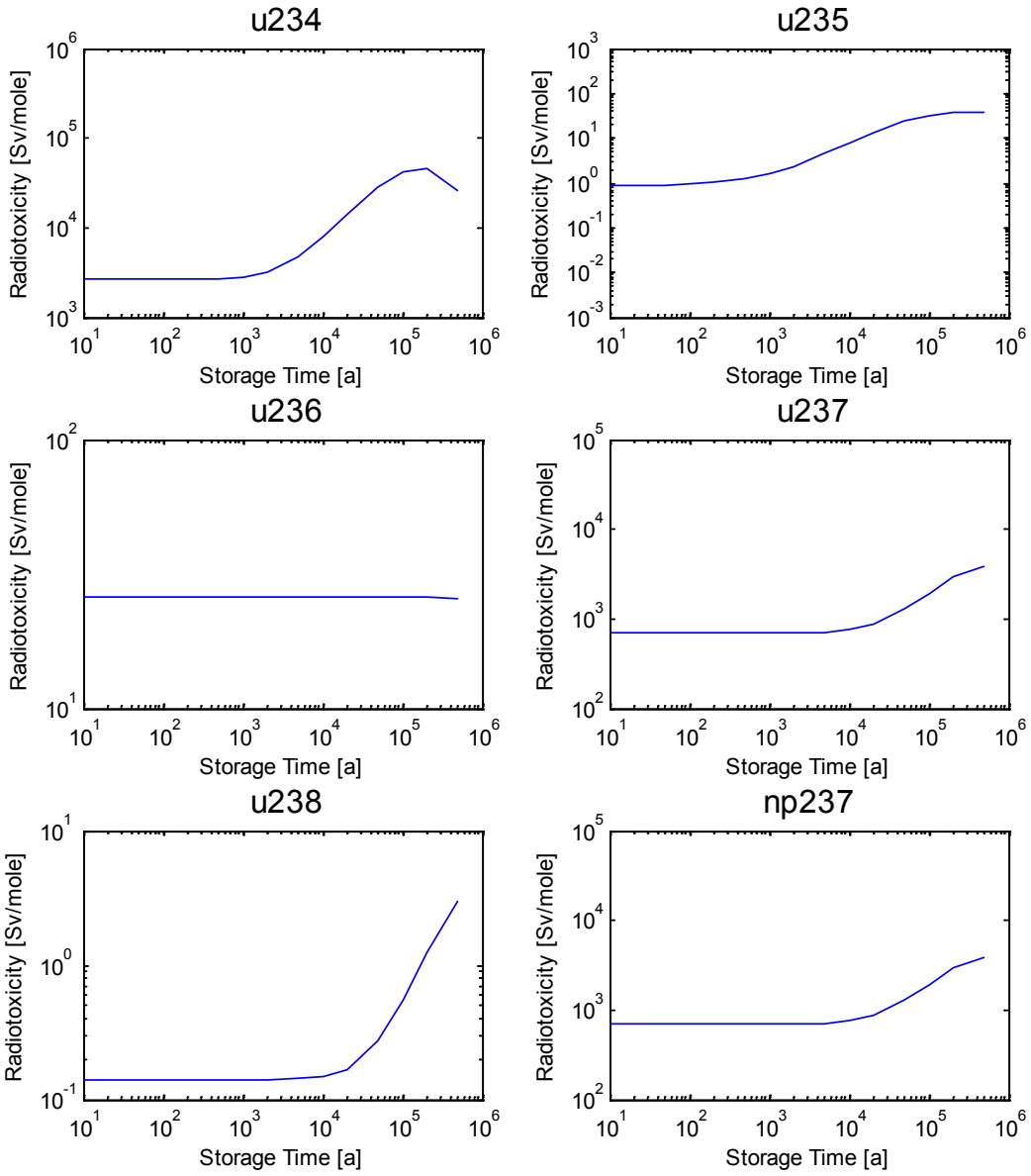

Figure D.2: *Radiotoxicity of U-234, U-235, U-236, U-237, U-238 and Np-237 and all their daughters.*

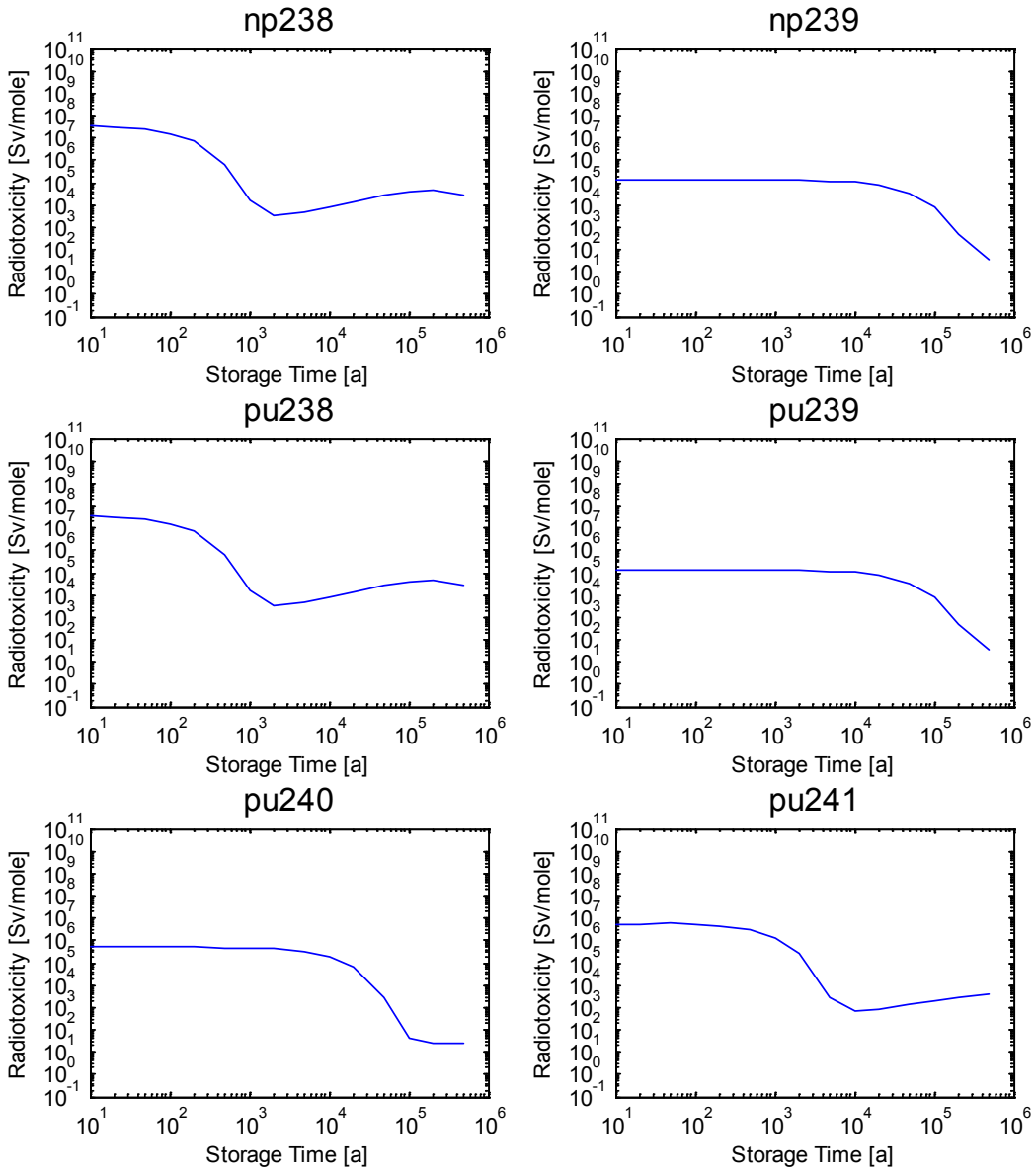

Figure D.3: *Radiotoxicity of Np-238, Np-239, Pu-238, Pu-239, Pu-240 and Pu-241 and all their daughters.*

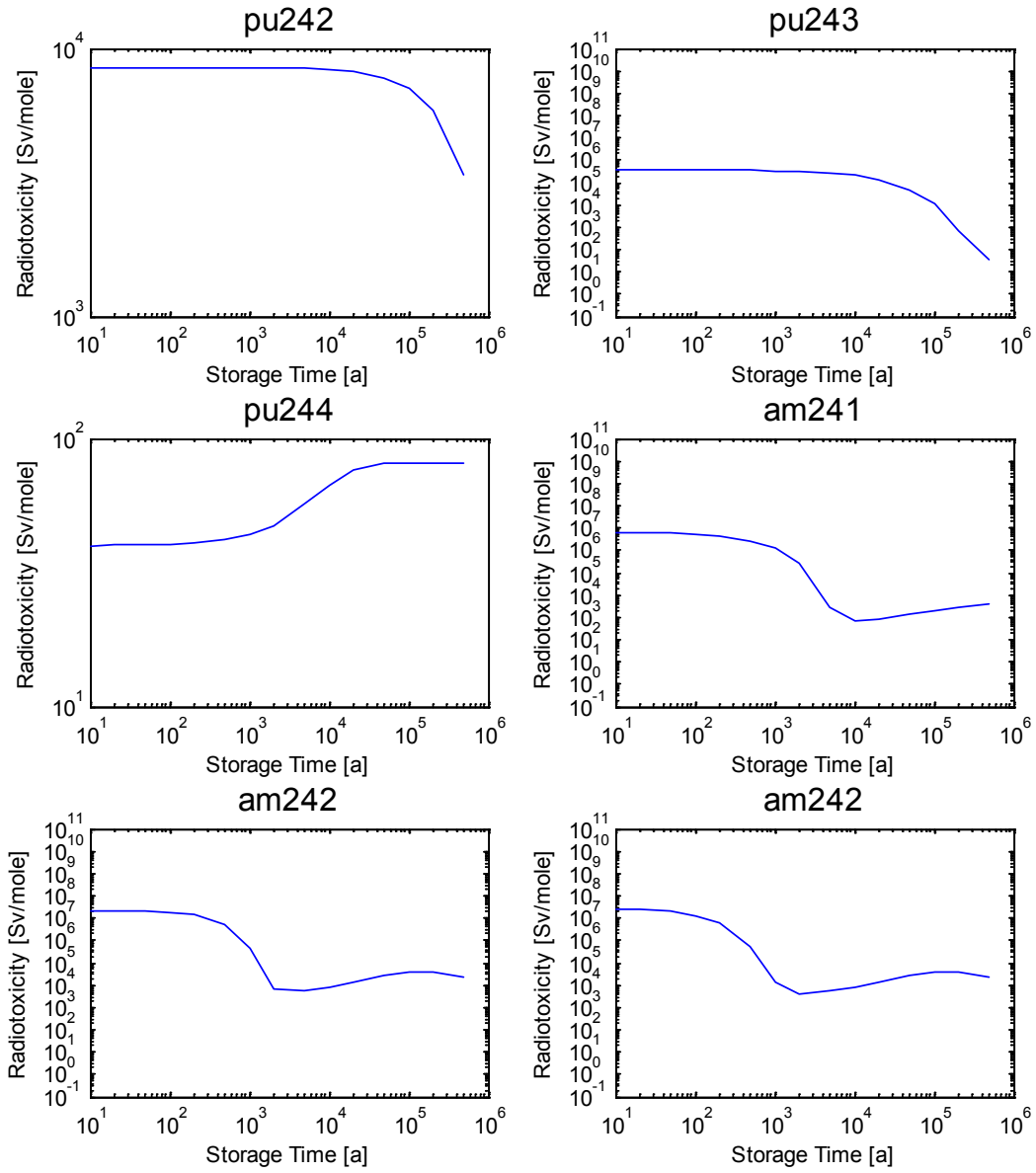

Figure D.4: *Radiotoxicity of Pu-242, Pu-243, Pu-244, Am-241, Am-242 and Am-242m and all their daughters.*

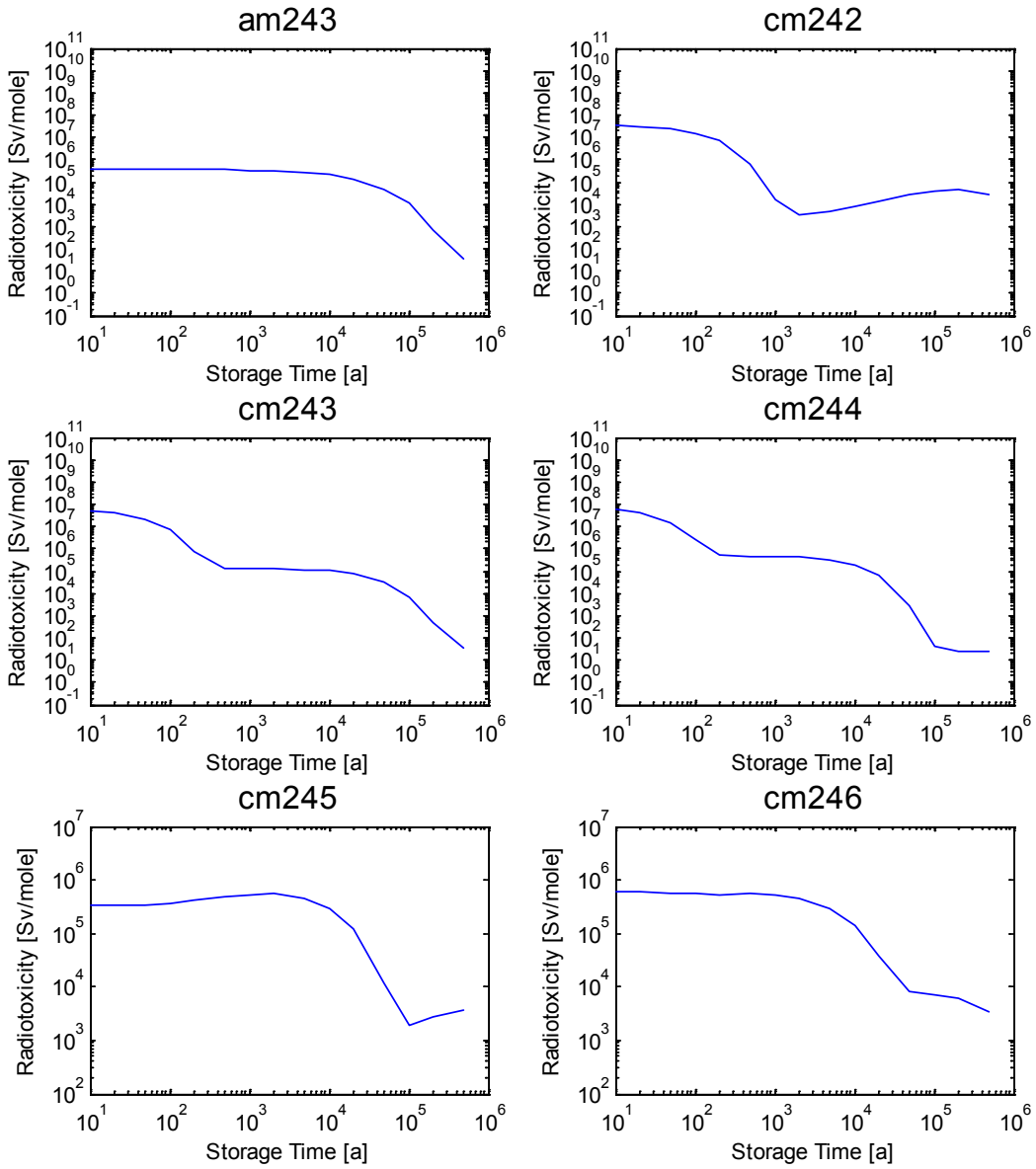

Figure D.5: *Radiotoxicity of Am-243, Cm-242, Cm-243, Cm-244, Cm-245 and Cm-246 and all their daughters.*

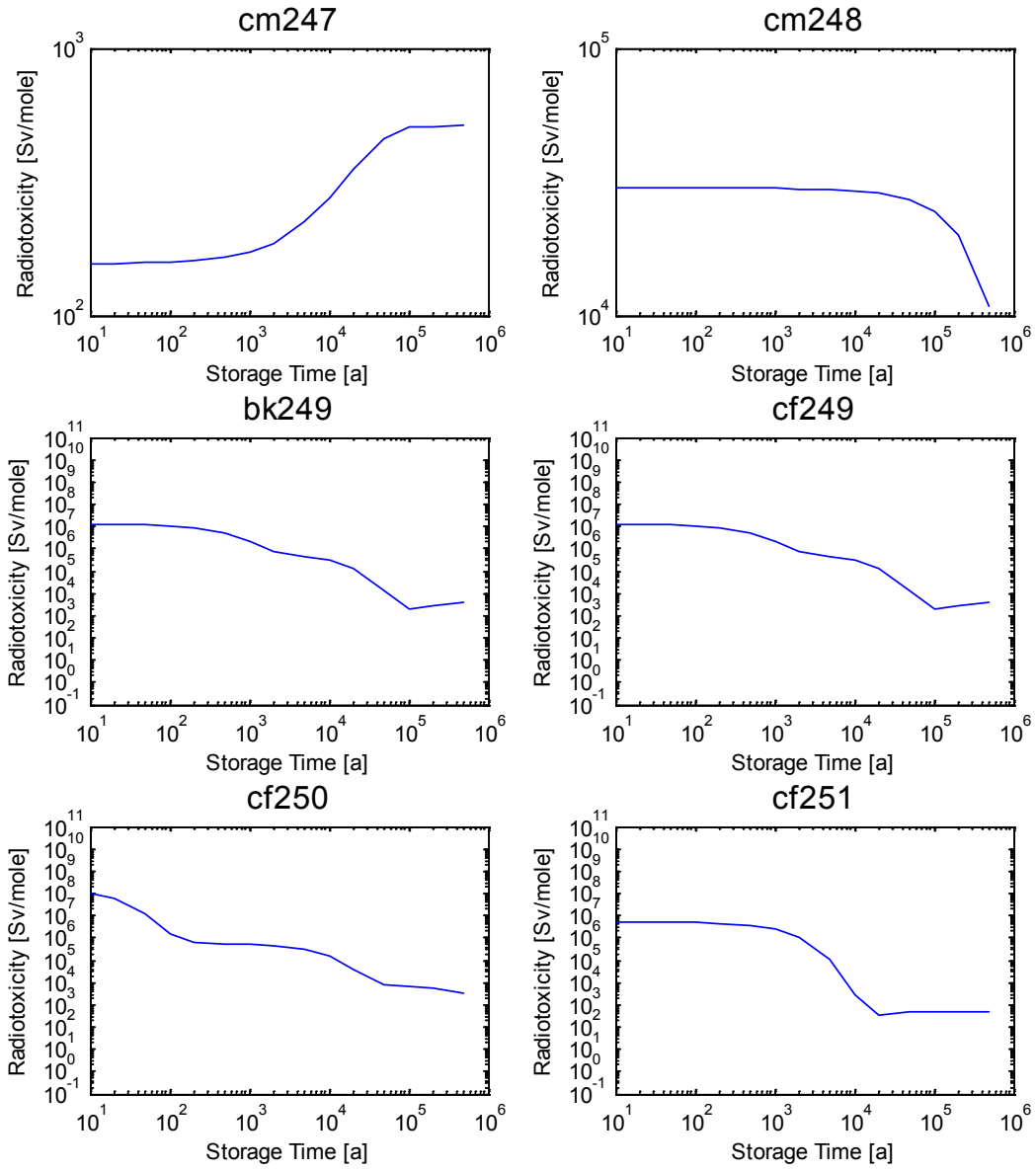

Figure D.6: *Radiotoxicity of Cm-247, Cm-248, Bk-249, Cf-249, Cf-250 and Cf-251and all their daughters.*

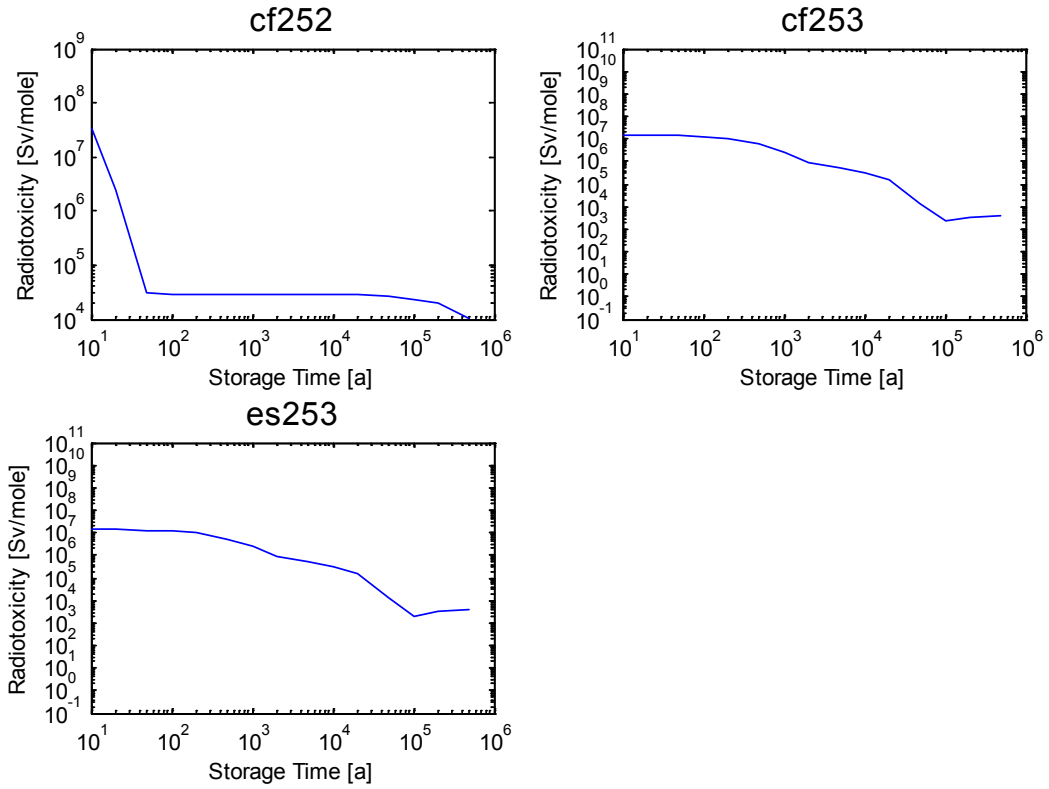

Figure D.7: *Radiotoxicity of Cf-252, Cf-253 and Es-253 and all their daughters.*